INVESTIGATING COTRANSLATIONAL INTEGRATION OF A MULTI-SPANNING MEMBRANE PROTEIN INTO THE ENDOPLASMIC RETICULUM MEMBRANE

A Dissertation

by

CANDICE GENE JONGSMA

Submitted to the Office of Graduate Studies of
Texas A&M University
in partial fulfillment of the requirements for the degree of

DOCTOR OF PHILOSOPHY

December 2008

Major Subject: Chemistry

INVESTIGATING COTRANSLATIONAL INTEGRATION OF A MULTI-SPANNING MEMBRANE PROTEIN INTO THE ENDOPLASMIC RETICULUM MEMBRANE

A Dissertation

by

CANDICE GENE JONGSMA

Submitted to the Office of Graduate Studies of
Texas A&M University
in partial fulfillment of the requirements for the degree of

DOCTOR OF PHILOSOPHY

Approved by:

Chair of Committee,	Arthur E. Johnson
Committee Members,	David H. Russell
	Frank M. Raushel
	J. Martin Scholtz
Head of Department,	David H. Russell

December 2008

Major Subject: Chemistry

ABSTRACT

Investigating Cotranslational Integration of a Multi-spanning Membrane Protein into the Endoplasmic Reticulum Membrane. (December 2008)

Candice Gene Jongsma, B.S.; B.S., Grand Valley State University

Chair of Advisory Committee: Dr. Arthur E. Johnson

Most membrane proteins in eukaryotic cells are co-translationally integrated into the endoplasmic reticulum (ER) membrane at aqueous pores termed translocons. During multi-spanning membrane protein (MSMP) integration, the nascent polypeptide is threaded into the translocon pore where each successive transmembrane segment (TMS) is moved laterally through the translocon into the bilayer. The hydrophilic polypeptide segments on each side of the TMS are alternately directed into either the aqueous cytosol or the aqueous ER lumen. How is the ER membrane permeability barrier maintained during this process?

For a single-spanning signal-cleaved membrane protein, nascent chain movement into the lumen occurs while an ion-tight ribosome-translocon junction prevents ion flow through the translocon pore. Prior to opening this junction to allow nascent chain movement into the cytosol, BiP (Hsp70 binding protein) effects closure at the lumenal end of the pore to maintain the membrane permeability barrier. To determine whether the ribosome and BiP alternately

mediate pore closure during the integration of a MSMP, integration intermediates with nascent chains of different lengths were prepared with a fluorescent probe positioned in the nascent chain far inside the ribosomal tunnel. Nascent chain exposure to the cytosol or lumen was then detected by the collisional quenching of the probe by iodide ions located on either the cytosolic or lumenal side of the membrane.

While the first TMS through the tunnel caused the ribosome-translocon junction to open, the second TMS elicited both the closure of this junction and the opening of the lumenal end of the pore. Movement of a third TMS through the tunnel caused the ribosome-translocon junction to re-open after closure of the lumenal end. Pore opening and closing occurred after each TMS was 4-7 residues from the peptidyltransferase center, irrespective of TMS location in the nascent chain. The ribosome treated all TMSs in the same manner, regardless of their individual sequence or their native orientation. The ER membrane permeability barrier is maintained by ribosome-translocon interactions during co-translational MSMP integration.

DEDICATION

To my Mother, for always supporting me, encouraging me,

and following me on my journeys.

ACKNOWLEDGEMENTS

I would like to thank my advisor, Dr. Johnson, for inviting me to join his research group even though he had (supposedly) already stopped accepting new graduate students in preparation for his retirement. I will always appreciate his decision to make an exception for me, allowing me to work for, and more importantly, learn from him and the other Johnson group members.

I would also like to thank my committee members, Dr. Russell, Dr. Raushel, and Dr. Scholtz, and substitute committee member, Dr. Pace, for their support throughout the course of this research.

I thank the members of the Johnson research group, both past and present, for their continued support, guidance, and encouragement during my time here. I owe many thanks to Yuanlong Shao and Yiwei Miao for their technical assistance and for ensuring I always had access to any reagents I needed. I've worked in a number of research labs, and the Johnson group members are some of the best I've had the pleasure of working with. There has always been someone willing to provide assistance, lend an ear, or just share a laugh.

Finally, thanks to my family for their love, encouragement, prayers, and support in everything I do. Above all, I thank God. I can do all things through Christ who strengthens me (Philippians 4:13).

TABLE OF CONTENTS

CHAPTER Page

LIST OF FIGURES

Page

LIST OF TABLES

CHAPTER I

INTRODUCTION

Cells are the structural and functional building blocks of all living organisms and fall into two general categories: prokaryotes and eukaryotes. Prokaryotes, which include bacteria and archaea, are unicellular organisms that are distinguished from eukaryotes on the basis of nuclear organization. Prokaryotes lack a nucleus and other intracellular organelles that are associated with eukaryotic cells, the eukaryotic cell (Fig. 1) is a highly organized complex of organelles enclosed within membranes. A defining feature of the eukaryotic cell is the nucleus, which contains the genetic material of a cell. Other organelles, such as the endoplasmic reticulum (ER), Golgi apparatus, and mitochondria are also found in eukaryotes. It has been suggested that eukaryotes evolved from prokaryotic history about 1.6-2.1 billion years ago (Knoll, 1992).

The ER is an extensive membrane network that serves many functions within the eukaryotic cell, including the facilitation of protein folding and the sorting of molecules targeted for specific destinations, such as the Golgi complex. The ER membrane is a single phospholipid bilayer that encloses an aqueous internal compartment known as the ER lumen. The ER membrane serves as a barrier separating the lumen from the cytoplasm. The lumen is a site

---

This dissertation follows the style of Cell.

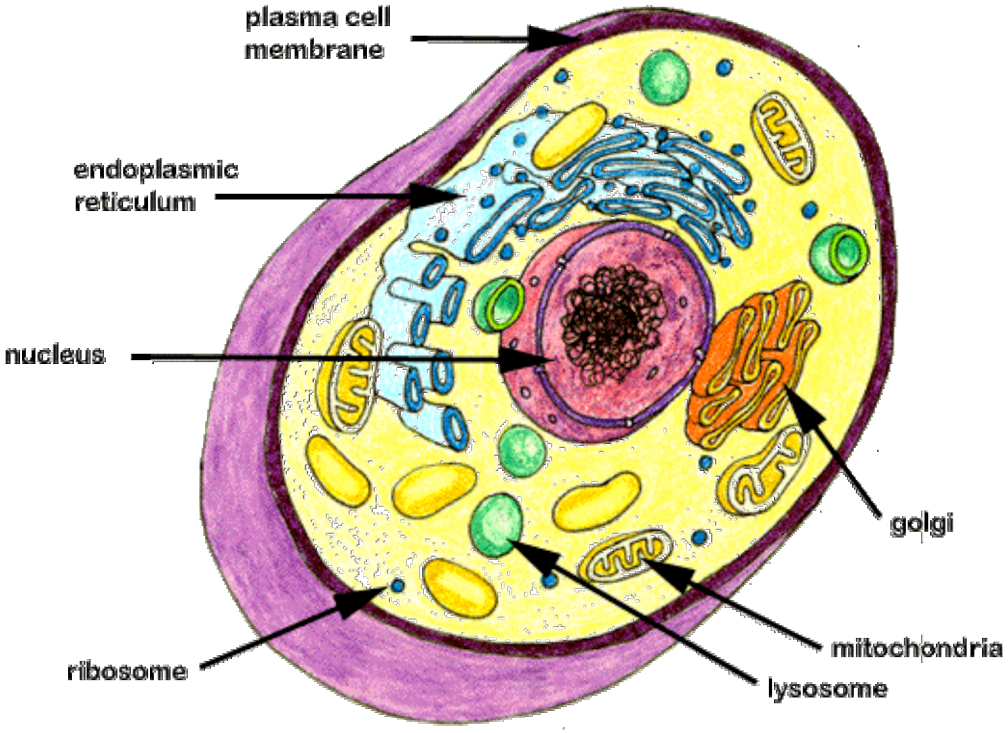

Figure 1. Eukaryotic cell. (http://www.yorku.ca/kdenning/++2140%202006-7/2140-17oct2006.htm: Denning, K., 2006) A eukaryotic cell is a highly organized membrane-bound structure containing a variety of organelles including the nucleus, ER, golgi apparatus, mitochondria, and ribosomes.

of protein modification in the cell, where cleavage of the signal sequence by signal peptidase (SP) and N-glycosylation by oligosaccharyltransferase (OST) are carried out. The lumen also functions as the primary storage location for intracellular calcium ions (Berridge, 2002; Koch, 1990). The concentration of calcium inside the ER lumen is several orders of magnitude greater than that in the surrounding cytoplasm (Demaurex and Frieden, 2003). These calcium ions function as potent second messengers when they are released from the ER lumen into the cytoplasm. Therefore, it is critical that the cell prevents the unregulated release of calcium from the ER during protein translocation through and integration into the ER membrane to avoid disrupting cell metabolism.

In eukaryotic cells, protein synthesis begins on free ribosomes that are dispersed in the cytoplasm. Approximately 30% of all proteins found in eukaryotic organisms are secretory or membrane proteins. Secretory proteins and soluble proteins localized in several organelles such as the ER lumen need to be transported across the eukaryotic ER membrane, while membrane proteins are inserted and integrated directly into the ER membrane. A protein that needs to be trafficked to the ER is recognized by the presence of a signal sequence, a short, hydrophobic stretch of amino acid residues (typically about 15-30 residues) that is usually located at the N-terminus of the polypeptide (Fig. 2). The signal sequence is bound to the signal recognition particle (SRP) upon

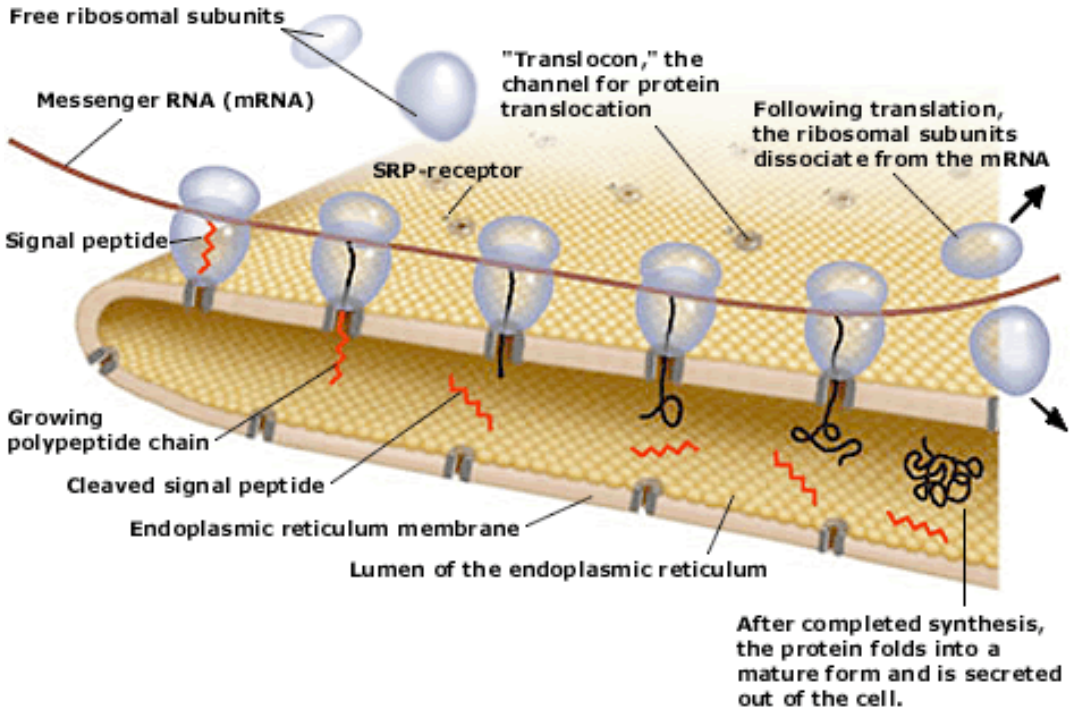

Figure 2. SRP-dependent targeting to the ER membrane. (http://nobelprize.org/nobel_prizes/medicine/laureates/1999/illpres/protein.html: Blobel, G., 1999) SRP recognizes and binds to a signal sequence, temporarily halting nascent chain elongation. The ribosome-nascent chain complex is directed to the translocon through interactions between SRP and the SRP-receptor. The ribosome engages with the translocon, SRP is released, and nascent chain elongation continues. After translation is complete, the ribosome disengages from the membrane and dissociates into its respective subunits.

emerging from the ribosome, and the SRP directs the ribosome•nascent chain complex to the ER membrane via an interaction with the SRP receptor (Walter and Johnson, 1994). The same translocation machinery is used to handle both soluble and membrane proteins. While protein trafficking is understood in general terms, the mechanisms involved are not well understood at the molecular level.

Membrane proteins play essential roles in a number of cellular functions such as signal transduction, proton pumping, and ion transport. Some membrane proteins associate peripherally with the membrane, while others, referred to as transmembrane (TM) proteins, span the entire bilayer (Fig. 3). TM proteins are amphipathic, meaning they contain hydrophobic and hydrophilic regions. The hydrophobic TM segments (TMSs) are embedded in and interact with the nonpolar core of the bilayer, while hydrophilic sections that loop between two successive TMSs extend into the aqueous regions located on either side of the membrane. TM proteins adopt particular orientations in the membrane because the cytoplasmic domains have different functions than the lumenal domains. TMSs that traverse the lipid bilayer fold into α helices to maximize the extent of hydrogen bonding within the nonaqueous membrane interior.

How are these large macromolecules able to be integrated into the ER membrane in the proper orientation, with hydrophilic domains located on both

sides of the membrane, without disrupting the permeability barrier and allowing leakage of small ions?

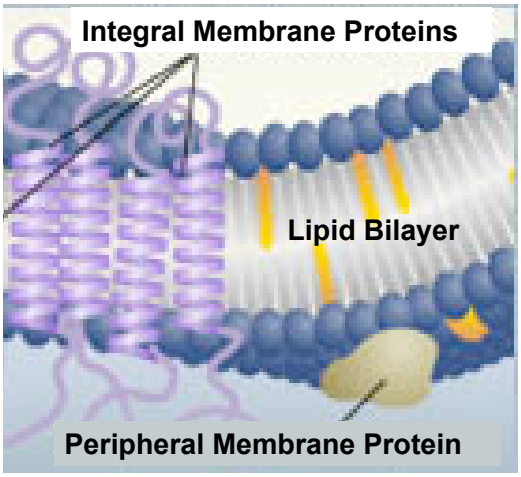

Figure 3. An integral membrane protein spans the phospholipid bilayer. (http://www.biology.arizona.edu/cell_bio/problem_sets/membranes/graphics/proteins.jpg: Grimes, W. and Lapointe, M., 2002) Transmembrane proteins contain hydrophobic domains that interact with the non-polar core of the bilayer and hydrophilic domains that extend into the aqueous regions located on either side of the bilayer.

Protein Biosynthesis

Central Dogma

Francis Crick first introduced the central dogma of molecular biology in 1958 (Crick, 1970). The genes of a cell contain genetic instructions for the two-step synthesis of proteins. The information encoded in genes can be converted from DNA to RNA through a process called transcription, and from RNA to protein through a process called translation (Fig. 4).

Transcription

Transcription is the process through which the DNA nucleotide sequence encoding a specific protein is copied, or transcribed, into RNA. Transcription begins by denaturing the double stranded DNA. The enzyme RNA polymerase moves along the double stranded DNA, opening and unwinding a small portion of DNA to expose the bases on the DNA strand. A single strand of DNA serves as the template for transcription. Incoming nucleotides are base-paired to the template, generating a single-stranded RNA molecule, or transcript, that is an exact complement to the template DNA strand. While the synthesized RNA performs a variety of functions, it is the messenger RNA (mRNA) whose base sequence is translated into a sequence of amino acids that comprise the protein.

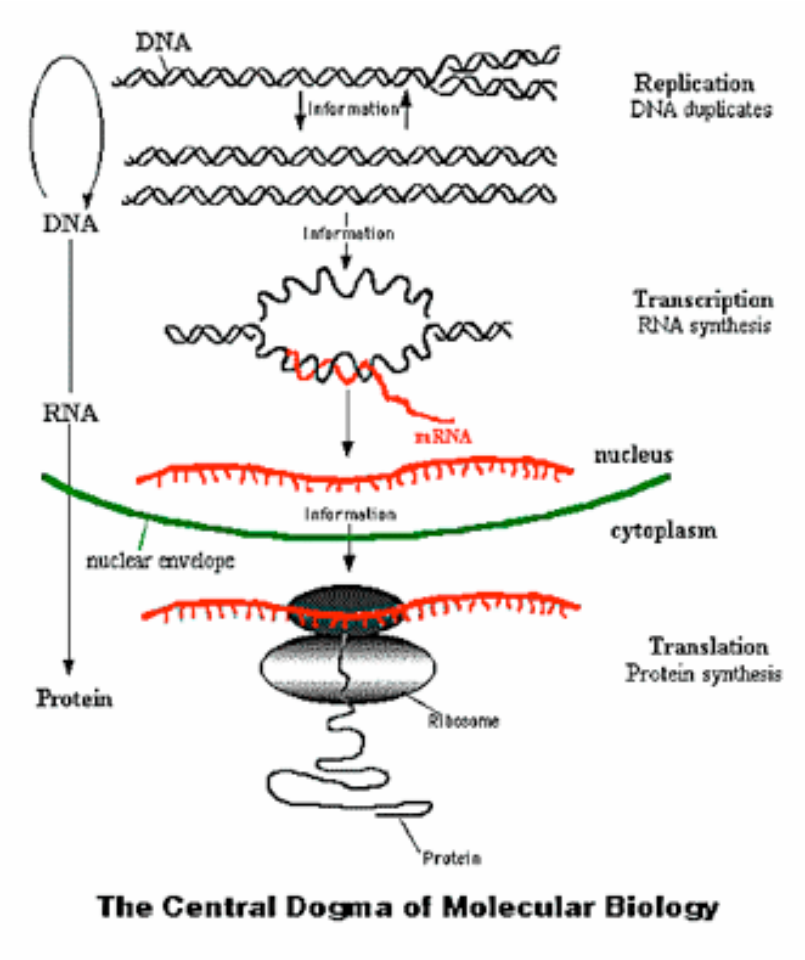

Figure 4. Central dogma of molecular biology. (http://www-stat.stanford.edu/~susan/courses/s166/central.gif: Holmes, S., 2007) The information contained in DNA is replicated and also transcribed into mRNA. Ribosomes read and translate the mRNA into a protein. This figure was downloaded from http://www-stat.stanford.edu/~susan/courses/s166/central.gif.

Translation

The information carried in a mRNA molecule is converted into a protein through a process called translation. The nucleotide sequence encoded by mRNA is read and translated into a “new language”, one based on amino acids instead of nucleotides, according to the rules of the genetic code. The base sequence in the mRNA molecule is read consecutively in groups of three. Each group of three consecutive RNA bases is called a codon and specifies a single amino acid. The genetic code is the key for identifying the codons and is used universally in all present-day organisms. The code is highly degenerate and many amino acids are identified by more than one codon.

Protein synthesis begins on free ribosomes in the cytoplasm of the cell. The 80S ribosome found in eukaryotes is composed of a smaller 40S subunit and a larger 60S subunit that associate during translation. The ribosome complex reads the mRNA in a 5’-to-3’ direction beginning with the start codon. The mRNA nucleotide sequence is translated into an amino acid sequence using transfer RNAs (tRNA) located in the cytoplasm. The tRNAs contain an anticodon that base-pairs with the codon on the mRNA chain, and this specifies a particular amino acid for addition to the growing nascent polypeptide chain. During translation elongation, the nascent chain is synthesized one amino acid at a time, beginning with the N-terminal end of a protein. The elongation cycle continues until a stop codon is reached, thereby halting translation. Termination

of translation causes the nascent polypeptide chain to be released from the tRNA and the ribosomal complex to dissociate back into its two respective subunits.

During translation the newly synthesized polypeptide chain is confined inside the ribosomal tunnel of the larger (60S) subunit. The ribosomal tunnel holds approximately 40 amino acid residues from the C-terminal end of the nascent chain (Blobel and Sabatini, 1970). As translation progresses, the nascent polypeptide chain is directed down the tunnel until the polypeptide chain exits the ribosome. It is only after the emergence of a signal sequence from the ribosome that the pathway of protein biosynthesis diverges from translation on free ribosomes to translation on membrane-bound ribosomes. The latter is the focus of this dissertation.

Protein Trafficking

SRP-Dependent Targeting to the ER Membrane

Nearly all eukaryotic secretory and membrane proteins are cotranslationally translocated across or integrated into the ER membrane, respectively, at sites termed translocons (Walter and Lingappa, 1986). These proteins are identified by a 15-30 residue signal sequence or a signal anchor at the N-terminus (von Heijne, 1985) that is recognized by the signal recognition particle (SRP). After the identifying signal sequence emerges from the ribosome, SRP binds to the signal sequence in the nascent chain and elicits a

temporary arrest of nascent chain elongation (Fig. 2). Interactions between the SRP and the SRP receptor, which is located at the ER membrane near the translocon, direct the SRP•RNC complex to the ER membrane (Gilmore et al., 1982a; Gilmore et al., 1982b; Johnson and van Waes, 1999; Meyer et al., 1982; Rapiiejko and Gilmore, 1997). SRP interacts with the SRP receptor in a GTP-dependent manner, initiating a series of reactions in which the signal sequence is released from the SRP, the SRP and SRP receptor move away from the ribosome, and the ribosome engages with the translocon. Protein synthesis is then resumed, and the nascent chain is directed into the translocon.

Translocon Components

The translocon is the site of secretory protein translocation across and membrane protein integration into the ER membrane (Walter and Lingappa, 1986). The core components of the mammalian translocon are thought to be the heterotrimeric Sec61 complex (Sec61$\alpha\beta\gamma$), the translocon-associated membrane protein (TRAM), and other translocon-associated proteins including the lumenal Hsp70 chaperone BiP (immunoglobulin heavy-chain binding protein) and SRP receptor (Johnson and van Waes, 1999; Nichitta and Blobel, 1990; Rapoport et al., 1996).

Cotranslational Translocation of a Secretory Protein

Blobel and Dobberstein first hypothesized that secretory proteins are translocated through the ER membrane into the lumen via an aqueous channel formed by integral membrane proteins (Blobel and Dobberstein, 1975). This hypothesis would be debated for nearly 20 years, until the first direct evidence supporting nascent chain occupancy an aqueous channel would be obtained (Crowley et al., 1994).

The secretory protein preprolactin (pPL) was used in early studies to glean information about the structure of the translocon and the cotranslational translocation process. Aminoacyl-tRNA analogs were used to site specifically incorporate water-sensitive fluorescent probes into the nascent chain of pPL during its synthesis by the ribosome (Crowley et al., 1994; Crowley et al., 1993).

Fluorescence lifetime measurements (see Ch. II for details) of the pPL translocation intermediates revealed that the fluorescent dye in the nascent chain was in an aqueous milieu inside the membrane-bound ribosome and the translocon (Crowley et al., 1994). Collisional quenching experiments utilizing iodide ions as hydrophilic collisional quenchers of fluorescence (see Ch. II for details) provided an independent confirmation that the nascent chain of the secretory protein passes through an aqueous pore in the translocon (Crowley et al., 1994). This result provided the first direct experimental evidence that the nascent secretory protein moves through the ER membrane via an aqueous

pore (Blobel and Dobberstein, 1975) rather than through the hydrophobic interior of the bilayer (Engelman and Steitz, 1981).

Additional collisional quenching experiments revealed that an ion-tight junction at the cytoplasmic end of the translocon pore is formed by the ribosome binding to the ER membrane (Crowley et al., 1993). The nascent chain is completely enclosed in an aqueous tunnel in the ribosome during cotranslational translocation (Fig. 5). Nascent chain movement into the cytoplasm is prevented by the docking of the ribosome on the translocon. Thus, the only direction that the nascent chain can move is down the ribosomal tunnel, where the nascent chain is then directed into the aqueous pore of the translocon. The quenching experiments also showed that the translocon pore is initially sealed at the lumenal end and is not opened until the nascent chain reaches a length of approximately 70 amino acids (Crowley et al., 1994). Therefore, it is possible for a secretory protein to be cotranslationally translocated across the ER membrane without being unnecessarily exposed to the cytoplasm.

The identity of the lumenal seal of the translocon was investigated by extracting all soluble lumenal proteins from microsomes and reconstituting them with purified proteins. These experiments revealed that BiP is both necessary and sufficient to mediate the sealing of the lumenal end of the translocon both in the ribosome-free state and when engaged with early translocation

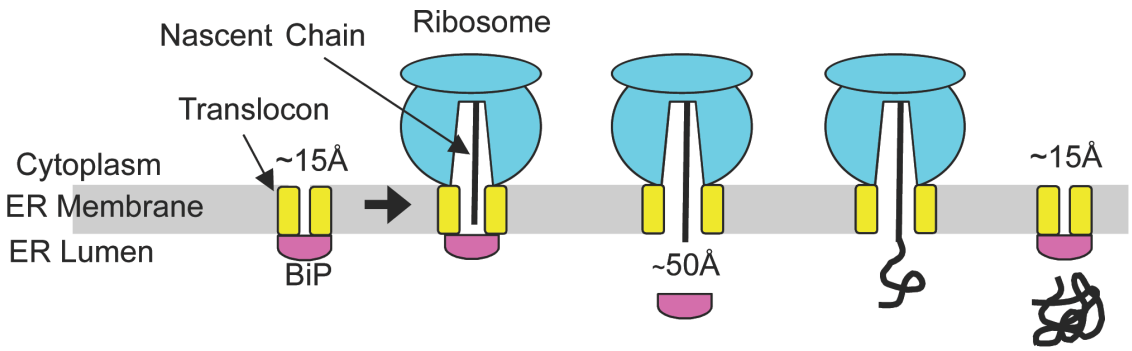

Figure 5. Cotranslational secretory protein translocation across the ER membrane. The ribosome-free translocon has a diameter of ~15 Å**.** A ribosome translating a secretory protein binds to the translocon of the ER membrane, forming an ion-tight seal. The translocon pore expands to an ID of ~50 Å and the secretory protein is cotranslationally translocated across the membrane. After translation is complete, the ribosome dissociates from the membrane and the translocon returns back to its ribosome-free state.

intermediates (<70aa) in a nucleotide-dependent manner (Hamman et al., 1998). The mechanism proposed for cotranslational translocation of a secretory protein across the ER membrane is shown in Figure 5.

The molecular dimensions of the translocon pore were determined by using collisional quenching agents of different sizes. Quenching agents were introduced into the interior of microsomes of intact, fully assembled translocation intermediates using pore forming proteins to determine which agents were small enough to enter the pore from the lumenal side and quench the fluorescence of a nascent chain probe located inside the ribosome on the cytoplasmic side of the ER membrane. The aqueous pore in a ribosome-bound, functioning translocon expands to an inner diameter of 40-60 Å (Hamman et al., 1997). In contrast, a ribosome-free translocon was determined to be much smaller, having an inner diameter of only 9-15 Å (Hamman et al., 1998).

Cotranslational Integration of a Single-spanning Membrane Protein

Translocation of a secretory protein required only an ion-tight ribosome-membrane junction to maintain the permeability barrier of the ER membrane. However, nascent membrane proteins must move TMSs laterally and allow egress of cytosolic domains from the ribosome-translocon pore, presumably by opening the ribosome-translocon junction without compromising the permeability barrier. When a TMS in a nascent chain reaches the translocon, it is retained at the translocon instead of continuing its passage through translocon pore into the

lumen (Do et al., 1996; McCormick et al., 2003). The ribosome-translocon seal must be broken to allow the cytoplasmic domains to move into the cytosol during cotranslational integration. This reality then raises the question: How is the permeability barrier of the membrane maintained during this process?

To address the mechanism of membrane protein integration at the ER membrane, previous studies have used a fusion protein, designated 111p, containing a pPL-derived signal sequence at the N-terminus to ensure proper targeting, followed by a lysine free stretch of pPL, and a single TMS derived from vesicular stomatitus G (VSVG) that is oriented $N_{lumenal}$-$C_{cytosolic}$ both in the native state and in 111p (Haigh and Johnson, 2002; Liao et al., 1997).

These experiments showed that the permeability barrier of the membrane is maintained by sealing the lumenal end of the translocon pore while the TMS is still far inside the ribosomal tunnel near the peptidyltransferase center (PTC) (Liao et al., 1997). Hence, it is the ribosome, not the translocon, that first recognizes a TMS and initiates a series of events converting the functional mode of the translocon from translocation to integration (Fig. 6). It was subsequently shown that BiP is responsible, either directly or indirectly, for sealing the lumenal end of the translocon pore (Haigh and Johnson, 2002). After the lumenal end of the pore has been sealed, the ion-tight ribosome-translocon seal at the cytosolic end of the pore is breached, presumably to allow the cytosolic domain of the nascent chain access to the cytoplasm (Haigh and Johnson, 2002; Liao et al., 1997). By sealing the lumenal end of the pore before opening the cytosolic end,

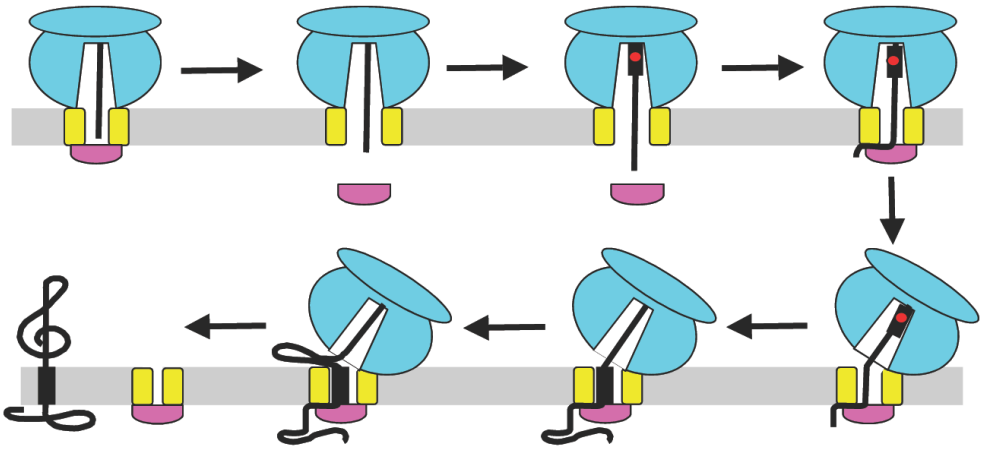

Figure 6. Cotranslational integration of a single-spanning membrane protein into the ER membrane. The RNC complex, containing a single TMS (black rectangle) with a fluorescent probe (red dot) incorporated into the nascent chain, is targeted to the translocon (yellow) during cotranslational integration. The lumenal end of the translocon pore is sealed by BiP (pink), either directly as depicted here or indirectly, prior to pore opening at the cytosolic end.

the system ensures that the integrity of the ER membrane is maintained. The proposed mechanism for cotranslational membrane protein integration of a single-spanning membrane protein into the bilayer is depicted in Figure 6.

How does the ribosome distinguish a nascent chain lacking a TMS and destined for translocation from a nascent chain containing a TMS and destined for integration into the membrane? Liao et al. (Liao et al., 1997) hypothesized that a TMS would fold into an α-helix when a TMS interacted with a weakly non-polar patch in the ribosomal tunnel. Fluorescence resonance energy transfer (FRET) was used to assess nascent chain conformation of a single-spanning membrane protein (Woolhead et al., 2004). The distance between an excited fluorescent donor dye and an acceptor chromophore can be measured by the extent of non-radiative energy transfer from the donor to the acceptor. The donor dye and acceptor dye were positioned on opposite sides of the TMS, and the efficiency of FRET between the two dyes was measured. Dye separation for a protein that is folded into an α-helix (1.5 Å per amino acid) is much less than that of a protein in a fully extended conformation (3.5 Å per amino acid). The FRET results showed that a TMS in a nascent membrane protein folds into a compact α-helix, or nearly so, when the TMS is far inside the ribosomal tunnel near the PTC (Woolhead et al., 2004). This folding is induced and stabilized by the ribosome, and the TMS retains the folded conformation as it moves through the ribosome, into the translocon, and enters into the membrane (Lin, 2008; Lin, unpublished data; Woolhead et al., 2004).

Additional insight was gained through photo-crosslinking studies in which a photoreactive probe was incorporated into the nascent chain of both a secretory and a membrane protein, and cross-linking to ribosomal proteins was examined. The data showed that a secretory protein photo-crosslinked to only one ribosomal protein having an apparent mass of approximately 40 kDa (Woolhead et al., 2004). In contrast, a single-spanning membrane protein photo-crosslinked to three different ribosomal proteins having apparent molecular masses of approximately 40, 18, and 7 kDa (Woolhead et al., 2004). The ribosomal proteins are believed to be L4 (40 kDa), L17 (18 kDa), and L39 (7 kDa) in eukaryotes (Ban et al., 2000).

These photo-crosslinking interactions coincide with the structural changes occurring at the translocon that were determined through fluorescence quenching. The BiP-mediated closure of the translocon pore at the lumenal end occurred when the TMS began to photo-crosslink to L17 (Woolhead et al., 2004). When the ribosome-translocon junction at the cytoplasmic end of the pore is opened, the TMS is then photo-crosslinked to L39 (Woolhead et al., 2004).

Based on the data obtained through TMS-dependent FRET, photo-crosslinking, and fluorescence collisional quenching experiments, a mechanism for the communication between the ribosome, nascent chain, and translocon has been proposed (Fig. 7). A weakly nonpolar surface in the ribosomal tunnel nucleates the folding of a TMS into a compact α-helix (or nearly so). This

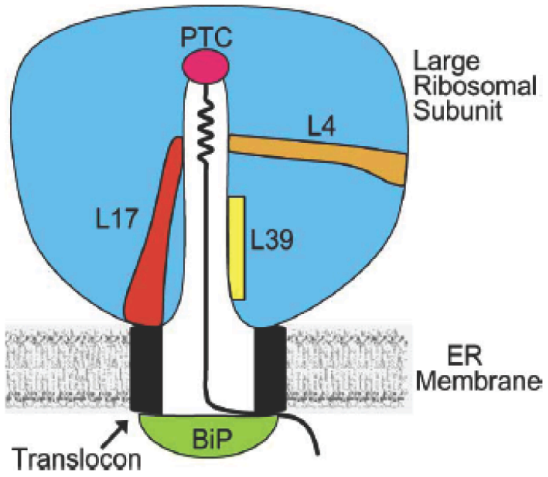

Figure 7. Large ribosomal subunit. The large ribosomal subunit is shown here. Both secretory and membrane proteins photo-crosslinked to L4. Membrane proteins also photo-crosslinked to L17 and L39. Reprinted with permission from Cell: (Woolhead et al., 2004), copyright Elsevier 2004.

appears to occur when the folded TMS reaches the tip of L17 in the nascent chain tunnel, and this in turn probably elicits a conformational change in L17 that extends to its domain located at the surface of the ribosome near the translocon. L17 then presumably interacts with a membrane-spanning protein, and this interaction triggers the BiP-mediated sealing of the lumenal end of the pore. As then nascent chain moves down the tunnel, the folded TMS next encounters the L39 protein. Interactions between the TMS and L39 result in the opening of the cytoplasmic end of the pore.

An Alternative Model Based on Cryo-EM and Crystal Structures

Despite the supporting evidence (Alder and Johnson, 2004; Crowley et al., 1994; Crowley et al., 1993; Haigh and Johnson, 2002; Hamman et al., 1997; Hamman et al., 1998; Liao et al., 1997; Woolhead et al., 2004), controversy still surrounds the mechanism by which the permeability barrier of the ER membrane is maintained (Rapoport, 2007; Rapoport et al., 2004). Cryoelectron microscopy (cryo-EM) studies have always detected a small “gap”, estimated to be as large as 20 Å (Beckman et al., 1997; Menetret et al., 2000) or as small as 12 Å (Osborne et al., 2005), between the translocon and the ribosome (Beckman, 2001; Morgan et al., 2002). It has therefore been inferred by these authors that the presence of a gap shows the ribosome does not form an ion-tight seal with the translocon as indicated by the fluorescence collisional quenching studies.

Based on a single crystal structure of a monomeric archaeal SecYEβ complex, an alternative model was described in detail in the reviews from Osborne et al., 2005 and Rapoport, 2007. In these models, ion flow is minimized due to a constriction in the translocon pore. The pore is purported to be formed from a single copy of the SecYEβ (which is presumably homologous to the mammalian Sec61 complex) (Osborne et al., 2005; Rapoport, 2007; van den Berg et al., 2004), that has an hour-glass shape with hydrophilic funnels on both sides of the constriction (Fig. 8). One funnel is exposed to the cytosol and the other funnel is sealed at the lumen by a short, helical "plug". The diameter of the pore ring in the crystal structure is thought to be too small for a polypeptide chain to pass through, so presumably the pore has some flexibility (Gumbart and Schulten, 2006; Haider et al., 2006; Saparov and al., 2007; Tian and Andricioaei, 2006) that allows it to expand at some point during translocation to accommodate the polypeptide chain. It is postulated that the insertion of the signal sequence into the translocon could force the translocon pore to widen to the appropriate size necessary to accommodate the polypeptide chain. When the polypeptide is being actively translocated through the pore "The pore ring would fit like a gasket around the translocating polypeptide chain, thereby restricting the passage of small molecules during protein translation. The seal would not be expected to be perfect…Leakage is probably compensated for by powerful ion pumps." (quoted text taken from Rapoport, 2007). The insertion of

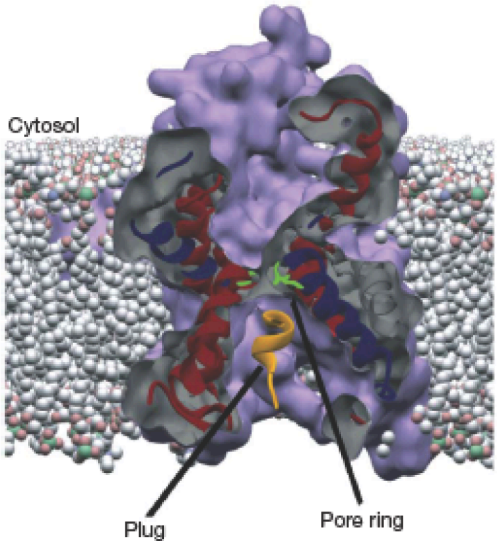

Figure 8. Cross-sectional view of a closed translocon channel. The pore is depicted having an hour-glass shape with a constriction in the center of the pore and a hydrophilic funnel at either end. The plug (in yellow) is in the center of the α-subunit. The pore-ring residues are shown in green. Reprinted with permission from Nature Reviews: (Rapoport, 2007), copyright Macmillan Publishers Ltd 2007.

the signal sequence would also destabilize plug interactions, causing the plug to move from the center of the pore into a cavity at the back of the molecule, thereby allowing the polypeptide to traverse the entire length of the pore.

The opposing views on ER membrane permeability that contrast so dramatically with the fluorescence studies may simply be explained by differences in samples that were examined. High-resolution crystal and cryo-EM studies require a detergent treatment to solubilize the translocon away from the membrane. Therefore, the samples used in the cryo-EM studies are lacking all lipids and also some translocon and translocon-associated proteins, such as TRAM. It is possible that the ribosome may not be able to form a seal with the translocon in the absence of these components. The crystal structure was also determined in the absence of the ribosome, the membrane, and translocon-associated proteins. Here, the crystal structure may not accurately represent the structure of an intact, fully-assembled and functional RNC•translocon complex. In stark contrast to the cryo-EM and crystal studies, the fluorescence collisional quenching experiments were performed using fully-assembled and intact samples maintained in aqueous solution under native conditions, thereby preserving the integrity of the translocons.

There are other discrepancies surrounding the interpretations of the cryo-EM and x-ray data as well. While one paper (van den Berg et al., 2004) and many reviews argue that the translocon pore is formed from only a single Sec61 complex, other papers (including some from the above labs) argue that the pore

is located at the interface of three or four complexes (Beckman et al., 1997; Beckman, 2001; Breyton et al., 2002; Manting et al., 2000; Morgan et al., 2002). There are also conflicting reports regarding the number of linkages connecting the ribosome to the translocon, with as few as one (Beckman et al., 1997) and as many as seven (Menetret, 2005) having been reported. In addition, the reported size of the gap observed between the ribosome and the translocon has shrunk from 20 Å (Menetret et al., 2000) to 12 Å (Osborne et al., 2005). Despite all of these uncertainties, these low resolution [15.4 Å (Beckman, 2001) to 27 Å (Menetret et al., 2000)] cryo-EM images have been used to develop detailed models that purport to explain the conformations and changes that occur to a functional translocon during translocation and membrane protein integration.

Specific Aims of This Dissertation

How is the permeability barrier of the ER membrane maintained when a MSMP containing both lumenal and cytosolic domains is threaded into the nonpolar bilayer during cotranslational integration? Previous work performed in this lab has shown that a single-spanning membrane protein elicits a series of changes at the translocon to maintain the barrier. The synthesis and movement of a single TMS into the ribosomal tunnel effected pore closure at the lumenal end of the pore, followed by pore opening at they cytosolic end. What is the gating mechanism when multiple TMSs are present?

Here I have used a fluorescence-based technique to directly and unambiguously examine the exposure of the nascent chain to the cytosol and the lumen at several different stages during the cotranslational integration of a MSMP into the ER membrane. In addition, several different TMSs were characterized to assess whether the ribosome recognizes length, sequence, hydrophobicity, and/or orientation during MSMP integration. While the first TMS results in pore opening at the cytosolic end of the pore, a second TMS reverses the gating process and results in pore opening at the lumenal end. The ribosome and translocon respond to a third TMS in the same manner as the first, closing the lumenal end and opening the cytosolic end of the pore. Thus, the translocon pore is alternately opened and closed as sequential TMSs of a MSMP are synthesized and moved into the translocon and membrane. At any given time during translation an ion-tight seal is maintained at one end of the pore, thereby ensuring that integrity of the membrane is always maintained.

CHAPTER II

METHODS AND MATERIALS

Plasmids and Mutagenesis

The plasmids used in this work were based on the original 111p construct that has been described in detail previously (Do et al., 1996; Liao et al., 1997). Plasmids containing multiple transmembrane segments with varying lengths of nascent chain between adjacent TMSs were prepared by and obtained from Dr. Peter McCormick. Site-directed mutagenesis was performed when necessary to add, delete, or move the lysine codon to a desired position in the protein.

Desalted and lyophilized DNA primers were designed using Vector NTI software and synthesized commercially by Integrated DNA Technologies, Inc (IDT) or Sigma Genosys. The primers were resuspended in double distilled water (ddH_2O) to a final concentration of 250 ng/μL. A typical PCR was performed in a total volume of 50 μL and contained 2.5 units Pfu Turbo DNA polymerase (Stratagene), 1x of the included corresponding Pfu buffer (Stratagene), 200 μM final concentration of dNTPs (Takara), 125 ng each of forward and reverse primer, 1 ng of plasmid DNA, and ddH_2O.

PCR reactions were carried out using a GeneAmp PCR System 9700 thermocycler. The reaction was first heated to 95°C for 30 s followed by 18 cycles of denaturing at 95°C for 30 s, annealing at 55°C for 60 s, and elongation

at 68°C for 10 min. A final extension for 5 min at 68°C and cooling to 4°C completed the program.

Following PCR, a Dpn1 (Promega) digestion was performed to digest the parental DNA template. PCR product (25 μL) was combined with 2 μL of Dpn1 and 3 μL of Dpn1's corresponding Buffer B (comes with the Dpn1). After the mixture was incubated at 37°C for 1.5 hr, 25 μL of the product was added to 100 μL of Top-10 competent *E. coli.* cells and incubated on ice for 10 min. A heat shock at 42°C for 60 s was performed, and then the sample was rapidly transferred back to ice for an additional 2 min. Next, 400 μL of LB media was added to the sample and the sample was incubated at 37°C for 1 hr on a shaker at 225 rpm. Then the culture was spread onto an LB ampicillin (40 mg/L) plate and incubated overnight at 37°C. Individual colonies were picked and placed in 5 mL of LB ampicillin agar and incubated overnight at 37°C, 225 rpm. The following day a pellet was prepared by centrifuging 1.5 mL of the mixture in a 1.5 mL microfuge tube for 3 min at 13000 rpm. The supernatant was aspirated, and the procedure was repeated one more time so that a total of 3 mL culture was used to form the pellet. Finally, the plasmid DNA was purified by following the procedures given in the *Qiagen Mini-prep Quick Kit (cat # 27106)* for use with a microcentrifuge. The plasmids were sequenced at the Gene Technologies Laboratory (Department of Biology, TAMU). The primers that were used to make the single-site mutations used in this dissertation are given in Table 1.

Table 1. Primers for site-directed mutagenesis.

Primer	Sequence	Mutation	Other Notes
FP212N28K	CCCGTCTGTCCCAAAGGGCCTG GCAAC	N28K	Complements RP212N28K
RP212N28K	GTTGCCAGGCCCTTTGGGACAG ACGGG	N28K	Complements FP212N28K
FP212K101N	CTACATCCTGCTCAACCTGGCC GTGGCC	K101N	Complements FP212K101N
RP212K101N	GGCCACGGCCAGGTTGAGCAGG ATGTAG	K101N	Complements RP212K101N
FP353KG144KA	GCCACCTTGGGCAAAGAAATTG CACTG	AAG to AAA	Complements RP353KG144KA
RP353KG144KA	CAGTGCAATTTCTTTGCCCAAGG TGGC	AAG to AAA	Complements FP353KG144KA
FP2TML41D99K	CCCACTACATCCATAAACTCTCC TCGGAAATG	D99K	Complements FP2TML41D99K
RP2TML41D99K	CATTTCCGAGGAGAGTTTATGGA TGTAGTGGG	D99K	Complements RP2TML41D99K
FP2TML41Q110K	GTTCAACGAATTTGATAAACGGT ATGCAACGGGCCAAGGG	Q110K	Complements RP2TML41Q110K
RP2TML41Q110K	CCCTTGGCCCGTTGCATACCGTT TATCAAATTCGTTGAA	Q110K	Complements FP2TML41Q110K
FP2TML41N124K	CATTACCATGGCCCTCAAAAGCT GCCATACCCGGCTG	N124K	Complements RP2TML41N124K
RP2TML41N124K	CAGCCGGGTATGGCAGCTTTTG AGGGCCATGGTAATG	N124K	Complements FP2TML41N124K
FP343L65KGKA	GCTTCTTTGCCACCTTGAAAGGT GAAATTGCACTGTG	AAG to AAA	Complements RP343L65KGKA
RP343L65KGKA	CACAGTGCAATTTCACCTTTCAA GGTGGCAAAGAAGC	AAG to AAA	Complements FP343L65KGKA
FPVSVG2I139K	CTGCGCAGACCCCTCAAGTCTA AAGCAAGC	I139K	Complements RPVSVG2I141K
RPVSVG2I139K	GCTTGCTTTAGAGTTGAGGGGT GTGCGCAG	I139K	Complements FPVSVG2I141K
FPTM2TM1I150K	GCAAGCTTTTTCTTTATCAAAGG CCTGATCATTGGAC	I150K	Complements RPTM2TM1IK
RPTM2TM1I150K	GTCCAATGATCAGGCCTTTGATA AAGAAAAAGCTTGC	I150K	Complements FPTM2TM1IK
FPOVK70I	GCTACATCCTGCTCATACTGGCC GTGGCCGACC	K70I	Complements RPOVK70I
RPOVK70I	GGTCGGCCACGGCCAGTATGAG CAGGATGTAGC	K70I	Complements FPOVK70I
FPOVK150N	GCAAGCTTTTTCTTTATCAACGG CCTGATCATTGGAC	K150N	Complements RPOVK150N
RPOVK150N	GTCCAATGATCAGGCCGTTGATA AAGAAAAAGCTTGC	K150N	Complements FPOVK150N

The PCR-based method described in detail by van den Ent and Lowe (van den Ent and Lowe, 2006) was used to move TMSs in their entirety to first create a construct containing two identical TMSs ($TM1_{L53}TM1$) and then to create a construct where the order of the TMSs has been reversed ($TM2_{L53}TM1$).

First, a PCR was set up containing a final concentration of 1x *Ex Taq*™ polymerase buffer Taq (Takara), 0.2 mM dNTPs (Takara), 2.5 u/μL ExTaq DNA polymerase (Takara), and 1 ng DNA plasmid $2TM_{L52}K2$. The forward primer 5'-CTGCAGCTGCGCACACCCCTCAACTCTATTGCAAGCTTTTTCTTTATCATAGGC-3' and the reverse primer 5'-GACGAAGTATCCGTGCAGAGAGGTGAGAACCAAGAATAGTCCAATGATCAGGCC-3' were added to final concentrations of 1 pmol/μL. The final volume was diluted to 50 μL using ddH_2O. Samples were first denatured for 2 min at 94°C. Then a cycle was repeated 30 times where samples were denatured for 30 s at 94°C, annealed for 30 s at 60°C, and elongated for 40 s at 72°C. A final extension at 72°C for 5 min followed by sample cooling to 4°C completed the PCR program. PCR products were purified using a *QIAquick PCR Purification Kit (Qiagen cat # 28106*). Purified PCR DNA was eluted in 30 μL of EB elution buffer (from kit).

A second PCR was set up containing a total volume of 50 μL. This PCR included 2.5 units Pfu Turbo DNA polymerase (Stratagene), 1x of the corresponding Pfu buffer (Stratagene), and 200 μM final concentration of dNTPs (Takara). Approximately 100 ng of purified PCR product from the previous PCR

and 1 ng of DNA plasmid $2TM_{L53}K2$ were added and the reaction was diluted to final volume using ddH_2O. Samples were denatured for 30 s at 95°C. A cycle consisting of denaturing for 30 s at 95°C, annealing for 60 s at 55°C, and elongating for 10 min at 68°C was repeated 35 times. After a final extension at 68°C for 5 min, the sample was cooled to 4°C to complete the PCR. The Dpn1 digestion and transformation were carried out exactly as previously described for site-directed mutagenesis, and the identity of the resulting plasmid was confirmed by sequencing at the Gene Technologies Laboratory (Department of Biology, TAMU).

The plasmid containing two TMSs whose order has been reversed ($TM2_{L53}TM1$) was prepared using the same PCR based method that has just been described. The first PCR contained the forward primer 5'-GAAATGTTCAACGAACTCGACAGGAGCTACATCCTGCTCAAACTGGCCGTGGCCGAC-3' and its complement 5'-CATGACTGCCCGCCGGAATTCTCGGTCGAGGGTGGTGGTGAAGCCCCCGAAGACC-3'. All other experimental conditions remained the same. The second PCR was identical to that previously described except that the newly made plasmid $TM1_{L53}TM1$ was used in place of $2TM_{L53}K2$. The resulting plasmid was $TM2_{L53}TM1$ and the identity was confirmed by sequencing. The primers used were synthesized commercially and PAGE-purified by IDT or Sigma Genosys.

PCR-generated Translation Intermediates

PCR was performed using a 5'-primer designed to include the start methionine and the SP6 promoter region and 3'-primers designed to generate DNA products of specified lengths. Primers were 20-30 base pairs in length and synthesized commercially by IDT. Table 2 gives the primers used for PCR to generate intermediates of varying lengths. A typical PCR was performed in a total volume of 50 μL. *Ex Taq*™ polymerase buffer Taq (Takara) and 2.5 mM dNTPs (Takara) were added to final concentrations of 1x and 0.2 mM, respectively. The forward and reverse primers were added to a final concentration of 1 pmol/μL each. The template DNA was added to a final concentration of 1 ng/μL. ExTaq DNA polymerase (Takara) was added to a final concentration of 2.5 u/μL. The total reaction volume was obtained by adding ddH_2O.

PCR samples were first denatured for 2 min at 94°C. Then a cycle where samples were denatured for 30 s at 94°C, annealed for 30 s at 60°C, and extended for 40 s at 72°C was repeated 30 times. A final extension at 72°C for 5 min followed by sample cooling to 4°C completed the PCR program.

PCR products were purified using a *QIAquick PCR Purification Kit (Qiagen cat # 28106*). Purified PCR DNA was eluted in 30 μL of EB elution buffer (from kit). Confirmation of successful PCR was obtained by running 5 μL of PCR product on a 1.6% (w/v) agarose/TAE [40 mM Tris-acetate and 1mM

Table 2. Primers for PCR-generated DNA fragments of different lengths.

Primer	Sequence	Template	Purpose
1335-EC	CCCAGTCACGACGTT GTAAAACG	Any	Forward Primer
RP111	ACAAGCTCGCGCAAT TAACCCTC	Any	Reverse Primer
2TML12-122	CAGAGAGGTGTAGAG GGTGGTGGTG	$2TM_{L12}K2$	$2TM_{L12}K2_{122}$
1450-CJ	GAAGTATCCGTGCAG AGAGGTGTAGAG	$2TM_{L12}K2$	$2TM_{L12}K2_{126}$
1459-CJ	GGGCCCAAAGACGAA GTATCC	$2TM_{L12}K2$	$2TM_{L12}K2_{130}$
2TML12-148	ACCTGAATCGTTACG GTCGACACTAG	$2TM_{L12}K2$	$2TM_{L12}K2_{148}$
2TML12-160	GTTGTTGTAATCAAC CACCATGGAGC	$2TM_{L12}K2$	$2TM_{L12}K2_{160}$
1451-CJ	CAGAGAGGTGTAGAG GGTGGTGGTG	$2TM_{L53}K2$	$2TM_{L53}K2_{163}$
1452-CJ	GTATCCGTGCAGAGA GGTGTAGAGGG	$2TM_{L53}K2$	$2TM_{L53}K2_{166}$
1459-CJ	GGGCCCAAAGACGAA GTATCC	$2TM_{L53}K2$	$2TM_{L53}K2_{171}$
1.5TML53-163	CAGGTTGCAGCCCGT GGGCC	$2TM_{L53}K1.5$	$2TM_{L53}K1.5_{163}$
1.5TML53-166	GAAGCCCTCCAGGTT GCAGC	$2TM_{L53}K1.5$	$2TM_{L53}K1.5_{166}$
1.5TML53-171	GTCGACACTAGTAAA GAAGCCCTCCAG	$2TM_{L53}K1.5$	$2TM_{L53}K1.5_{171}$
TM1TM1-159	CAGAGAGGTGAGAAC CAAGAATAGTCC	$TM1_{L53}TM1K$	$TM1_{L53}TM1_{159}$
TM1TM1-162	GTATCCGTGCAGAGA GGTGAGAACC	$TM1_{L53}TM1K$	$TM1_{L53}TM1_{162}$
TM1TM1-167	GGGCCCAAAGACGAA GTATCCG	$TM1_{L53}TM1K$	$TM1_{L53}TM1_{167}$
TMTM1-91	GAATTCTCGGTCGAG GGTGGTGG	$TM2K_{L53}TM1$	$TM2_{L53}TM1_{91}$
TMTM1-94	TGCCCGCCGGAATTC TCGGTA	$TM2K_{L53}TM2$	$TM2_{L53}TM1_{94}$
TMTM1-99	GTGGGACACCATGAC TGCCCG	$TM2K_{L53}TM3$	$TM2_{L53}TM1_{99}$
TM1TM1-159	CAGAGAGGTGAGAAC CAAGAATAGTCC	$TM2_{L53}TM1K$	$TM2_{L53}TM1_{163}$
TM1TM1-162	GTATCCGTGCAGAGA GGTGAGAACC	$TM2_{L53}TM1K$	$TM2_{L53}TM1_{166}$
TM1TM1-167	GGGCCCAAAGACGAA GTATCCG	$TM2_{L53}TM1K$	$TM2_{L53}TM1_{171}$
1462-CJ	GTACCGCTCGATGGC CAGGAC	$3TM_{L12,17}K3$	$3TM_{L12,17}K3_{159}$
1463-CJ	CACCACCACGTACCG CTCGAT	$3TM_{L12,17}K3$	$3TM_{L12,17}K3_{162}$
1464-CJ	GTCGACACTAGTGCA CACCACCAC	$3TM_{L12,17}K3$	$3TM_{L12,17}K3_{167}$
1462-CJ	GTACCGCTCGATGGC CAGGAC	$3TM_{L12,67}K3$	$3TM_{L12,67}K3_{209}$
1463-CJ	CACCACCACGTACCG CTCGAT	$3TM_{L12,67}K3$	$3TM_{L12,67}K3_{212}$
1464-CJ	GTCGACACTAGTGCA CACCACCAC	$3TM_{L12,67}K3$	$3TM_{L12,67}K3_{217}$

EDTA (pH 8.0)] gel containing ethidium bromide (10 mg/mL) under a constant voltage of 120 Volts.

Preparation of Lys-tRNA^{Lys}

Yeast Lys-tRNA^{Lys} and εNBD-Lys-tRNA^{Lys} were purified and prepared by Yuanlong Shao and Yiwei Miao as previously described in detail (Crowley et al., 1993, Johnson et al., 1976). The extent of NBD modification of the side chain amino group of lysine in εNBD-Lys-tRNA^{Lys} was determined by paper electrophoresis (Johnson et al., 1976).

In vitro Transcription

Typically, a 100 μL in vitro transcription reaction consisted of 20 μL DNA (see above) and the following reagents added to the final concentrations specified: 80 mM HEPES (pH 7.5); 16 mM $Mg(OAc)_2$; 2 mM Spermidine; 10 mM DTT; 3 mM each of ATP; CTP, UTP, and GTP; 0.5 mM Diguanosine Triphosphate [GpppG] (Amersham); 0.5 units / μL RNasin™ (Promega); 3 μL purified SP6 RNA polymerase; 0.005 units / μL Pyrophosphatase. Samples were incubated at 37°C for 90 min. Then an additional 3.2 μL of 100 mM GTP was added, and samples are incubated for an additional 40 min. After the incubation was complete, the RNA was precipitated by adding 13.3 μL of 3 M NaOAc (pH 5.2) and 340 μL of 100% ethanol. Samples were incubated on ice for a minimum of 1 hr. Samples were spun at 4°C for 20 min at 14,000 rpm in a

Beckman Coulter microfuge. The supernatant was aspirated and the pellets are washed with 1 mL of 70% (v/v) ethanol. Samples were spun for an additional 10 minutes at 4°C, the supernatant was aspirated, and the pellets were dried on a speed vac for 30 minutes. The dry pellets were resuspended in 100 μL of TE Buffer [10 mM Tris-HCl (pH 7.5)/ 1 mM EDTA (pH 7.5)]. The homogeneity of the transcription products was confirmed on a 1.8 % agarose/TAE gel. The prepared mRNA was frozen using liquid nitrogen and stored at -80°C for future use in in vitro translations.

In vitro Translations

Proteins were synthesized by in vitro translation in the presence of SRP and salt-washed ER microsomes (KRMs). The total translation volume for collisional quenching experiments was 500 μL. The translation mixture was prepared in a 1.5 mL microfuge tube and included the following: 100-130 mM KOAc (pH 7.5) (optimize); 20 mM HEPES (pH 7.5); 3.0-3.5 mM $Mg(OAc)_2$ (optimize); 1 mM DTT; 0.2 mM Spermidine; 8 μM SAM (S-Adenoysyl-Methionine); 1 X protease inhibitors (PIN); 0.2 units/μL RNasin (Promega); 2 μM EGS-K/EGS-M (energy generating system containing 375 μM of each of the 20 amino acids with the exception of lysine (K) or methionine (M), 120 mM creatine phosphate, and 0.12 units/μL creatine phosphokinase); 60-80 μL (optimize) wheat germ (WG); 40 nM SRP; 80 eqs KRMs; 40 μL mRNA; and 300 pmol εNBD-Lys-$tRNA^{Lys}$ or [^{14}C]Lys-$tRNA^{Lys}$.

The SRP and KRMs were prepared in-house as described before (Walter and Blobel, 1983). The WG was prepared as previously described (Erickson and Blobel, 1983). For translations which would be analyzed by SDS-PAGE, EGS lacking methionine (EGS-M) was sometimes instead of EGS-K, and 0.1 μCi/μL [^{35}S]methionine was also added. The protease inhibitors (PIN) were prepared in a 200x stock as already described (Erickson and Blobel, 1983). Before the addition of the mRNA, tRNA, and the [^{35}S]-Met when necessary, the reaction was incubated at 26°C for 7 min to allow for unlabeled translation of any endogenous mRNAs. After the addition of the mRNA and tRNA, reactions were incubated at 26°C for 40 minutes. When working with longer nascent chain lengths (171 amino acid residues and longer), the mRNA and tRNA were not added until after the translation had proceeded for 5 min.

Trichloroacetic Acid Precipitation

The in vitro translations were routinely analyzed by hot trichloroacetic acid (TCA) precipitation to quantify the amount of acid-precipitable radioactivity in a sample. Typically, a 2 μL aliquot of translation mixture was mixed with 1 mL of 10% (w/v) TCA/ 3% (w/v) casamino acids (CAA) in a 13 x 100 mm glass test tube. The sample mixture was then incubated at 85°C for 10 min and subsequently cooled on ice for an additional 2 min. The heating hydrolyzed any RNA molecules while precipitating the polypeptides. The samples were vortexed and filtered under vacuum through a 25 mm Metricel nitrocellulose

membrane filter (45 um pore size, Gelman Sciences) that had been prewashed with 3 mL cold 5% (w/v) TCA. The precipitate on the filter was washed with 3 mL cold 5% (w/v) TCA a total of three times prior to drying. The filters were dried under a heat lamp for 10 min, resuspended in PPO/POPOP/toluene scintillation cocktail, and counted in a liquid scintillation counter (Beckman).

SDS-PAGE

The translation products were resolved by SDS-PAGE using gels that were 14 cm high x 19 cm wide x 0.8 mm thick. The stacking portion of the gel was prepared with 4% polyacrylamide, 60 mM Tris-HCl (pH 6.8), 0.1% (w/v) SDS, 360 mM sucrose, 0.05% (v/v) N, N, N', N'-tetramethylethylenediamine (TEMED), and 0.08% (w/v) ammonium persulfate (APS). The resolving gel, containing a 10-15% (w/v) linear gradient of polyacrylamide, was made using 400 mM Tris-HCl (pH 8.8), 0.08% (w/v) SDS, 0.02% (v/v) TEMED, and 0.08% (w/v) APS mixed with a stock solution (Biorad) of 30% (w/v) acrylamide / 0.8% (w/v) bisacrylamide. All reagents were obtained from Sigma unless noted.

Samples were prepared for electrophoresis by resuspension in sample buffer containing 120 mM Tris-base, 3.6% (w/v) SDS, 7.5 mM EDTA, 125 mM DTT, 15% (v/v) glycerol, and a small amount of bromophenol blue. The samples were heated for 5 min at 95°C, and then briefly centrifuged to collect the sample in the bottom of the microfuge tube. The gel was submerged in running buffer containing 50 mM Tris-HCl (pH 8.8), 400 mM glycine, and 0.1% (w/v) SDS.

Twenty μL aliquots of each sample were then loaded into wells located in the stacking portion of the gel and having the dimensions 2 cm high x 0.5 cm wide x 0.8 mm thick. The gel was run at a constant current of 15 mA for 40 minutes during which time the samples moved through the stacking portion of the gel, followed by a constant current of 30 mA for 2 hours and 20 minutes while the samples moved through the resolving portion of the gel.

After the run was completed, the gel was placed in a destaining solution containing 10 % (v/v) glacial acetic acid and 35% (v/v) methanol. The gel was destained for a minimum of 20 minutes. After destaining, the gel was rinsed with water for 10 minutes to remove the acetic acid. Then the gel was placed on a piece of 3MM paper (Whatman) and dried for 40 minutes at 80°C in the gel dryer. The dried gel was taped inside a cassette and exposed to a phosphorimaging screen (Kodak) for a minimum of one night. The image of the gel was visualized using a phosphorimager (Pharos FX Plus Molecular Imager, BioRad) and a corresponding software package (Quantity One version 4.6.5, BioRad).

Carbonate Extraction

The standard method to determine whether a protein has been integrated into a membrane is to perform an alkaline carbonate extraction (Fujiki et al., 1982). If a protein is insoluble in alkaline buffers (pH 11.5), the protein is considered to be membrane-integrated.

After translation, samples were spun through a sucrose cushion buffer as described earlier. Samples were resuspended in 100 mM Na_2CO_3 (pH 11.5). Samples were then incubated on ice for 30 min. After incubation the samples were sedimented through an alkaline cushion buffer [0.5 M sucrose/ 100 mM Na_2CO_3(pH 11.5)] at 4°C, 100,000g for 20 min in a TLA 100 rotor using a Beckman Optima TL Ultracentrifuge. The membrane pellet and supernatant fractions were separated and analyzed by SDS-PAGE.

Preparation for Fluorescence Measurements

To perform collisional quenching experiments and lifetime measurements, MSMP integration intermediates were generated by in vitro translation using the conditions described above. Each experiment required two reactions. The first reaction, designated the "sample", was performed in the presence of εNBD-[^{14}C]Lys-tRNA^{Lys}. The second reaction, termed the "blank", was performed in the presence of unmodified [^{14}C]Lys-tRNA^{Lys}. After translation was complete samples were treated with a high salt wash (or sometimes a Proteinase K (ProK) and/or nuclease treatment) prior to sample purification by gel filtration chromatography to remove unincorporated fluorphores and improperly targeted material.

A high salt wash was performed to remove adsorbed salt-sensitive NBD-containing material from the integration intermediate before the intermediate moves into Buffer A. Gel filtration columns were pre-loaded with 2 mL of high

salt Buffer A (500 mM KOAc (pH 7.5)/ 20 mM HEPES/ 3.2 mM $Mg(OAc)_2$). After translation was complete, additional KOAc was added to the integration intermediates to a final concentration of 500 mM. The reactions were incubated on ice for 10 min before being loaded onto the gel filtration columns.

Some samples received a more stringent treatment after translation was complete. Instead of receiving a high salt wash, some samples were treated with ribonuclease, followed by proteinase K, as described next.

Polysome formation was minimized in some samples by performing a nuclease treatment that cleaved mRNA that were not protected by ribosomes, degrading polysomes to monosomes (Wolin and Walter, 1988). Staphylococcus aureus ribonuclease (100 units) and 1 mM $CaCl_2$ were added to samples at the conclusion of the translation incubation, and the samples were incubated for another 10 min at 26°C.

An optional protease treatment to digest polypeptides exposed to the cytosol could be performed using Proteinase K (ProK, Sigma). The ProK was added in a ratio of 20 μg ProK per 1 mL translation, and samples were incubated on ice for 20 min. PMSF was added to a final concentration of 1 mM to quench the ProK, and samples were incubated on ice for an additional 20 min.

Gel Filtration Chromatography

Gel filtration chromatography was used to purify integration intermediates. Typically, a 500 μL translation incubation was loaded onto a Sepharose CL-2B (Sigma Aldrich) gel filtration column [0.7 x 50 cm (BioRad)] equilibrated at 4°C with buffer A. The flow rate was approximately 2-3 drops per minute, and 11-12 drop fractions containing approximately 550 μL were collected in 13 x 100 mM glass test tubes using a fraction collector (Gilson FC 203B). The sepharose CL-2B was replaced regularly, typically after every 4 experiments, to ensure that the samples continued to be well purified. Proper pouring of the column could be visually assayed by loading a mixture containing blue dextran and potassium ferricyanide onto the column. The mixture separates into two colors, blue and yellow, when run over a properly poured column. The nascent polypeptide•ribosome•membrane complexes were eluted in the void volume. The fractions containing the RNC complexes were identified by measuring the light scattering at λ_{ex} 468 nm and λ_{em} 485 nm. Two fractions, giving a total sample volume of approximately 1.1 mL, were pooled together for use in the collisional quenching experiments.

Steady-state Fluorescence Spectroscopy

Fluorescence measurements were made on an SLM Aminco 8100 spectrofluorometer using a 450 watt xenon arc lamp as the light source. The excitation light passed through a double monochromator to reach the samples

housed in a chamber cooled to 4°C using a water bath. Nitrogen was flushed through the chamber to prevent condensation from forming on the walls of the quartz 4 mm x 4 mm microcuvettes (Starna Cells, Inc.). A single emission monochromator and a Peltier-cooled PMT housing completed the instrumental setup.

To eliminate any background signal and light scattering when measuring the observed NBD fluorescence intensity, readings of both the sample and the blank were taken using an excitation wavelength of 468 nm and an emission wavelength of 485 nm with a 4nm bandpass. Five successive 5-second integrations of emission intensity were recorded and averaged to give the emission intensity. The sample with the higher reading was diluted using buffer A until the same emission intensities for both the sample and the blank were obtained at 485 nm. Samples were allowed to equilibrate to 4°C for 5 min before any measurements were obtained.

Collisional Quenching of NBD with Iodide Ions

Aliquots (250 μL) of both the sample and blank were placed into 4 microcuvettes, designated S_0-S_4 and B_0-B_4 respectively. The NBD emission intensity was measured using excitation and emission wavelengths of 468 nm (4 nm bandpass) and 530 nm (4 nm bandpass), respectively, for all of the cuvettes. The initial net NBD emission intensity (F_0) was obtained by subtracting the blank signal from the sample signal (S_0 - B_0, etc.).

Next, each cuvette was given an equal volume (10 μL), but differing concentration, of iodide ions. The final KI concentrations after addition to the cuvettes ranged from 0 to 38 mM. The KI was diluted using KCl to maintain a constant ionic strength. The reducing agent $Na_2S_2O_3$ was added to the KI stock to a final concentration of 2 mM, before diluting with KCl, to minimize I_2 formation. The cuvettes were thoroughly mixed, equilibrated to temperature, and the net NBD emission intensity (F) was again measured. Melittin was then added to each cuvette as described below, and the fluorescence intensities were measured for a third time.

The data obtained during the examination of the steady-state collisional quenching of NBD fluorescence were analyzed using the Stern-Volmer equation. The extent of fluorescence quenching is dependent upon the number of collisions, and hence is directly proportional to the concentration of quencher as described by the Stern-Volmer equation:

$$(F_0/F) - 1 = K_{SV}\,[Q] = k_q\tau_0\,[Q] \quad (1)$$

where F_0 is the initial net fluorescence intensity in the absence of iodide ions, F is the net emission intensity in the presence of quencher, k_q is the bimolecular quenching constant, τ_0 is the lifetime of the fluorophore in the absence of quencher, and [Q] is the concentration of quencher. The Stern-Volmer constant, K_{SV}, equals $k_q\tau_0$. A linear least-squares best-fit graphical analysis of the data in which the line was constrained to go through the origin (0, 0) was performed to determine the slope (K_{SV}), which is proportional to the extent of quenching.

Melittin Treatment

The honey bee toxin melittin (Sigma) was used to induce pore formation in the ER membrane. Melittin (MLT) was diluted using ddH_2O, divided into 50 μL aliquots (enough for 1 quenching experiment), and stored at -80°C until ready for use. MLT was added to each sample to a final concentration of 5 μM and mixed thoroughly. The samples were incubated for 30 min at room temperature in the dark before being equilibrated to 4°C in the SLM cuvette turret and subsequent measurement of the net fluorescence emission intensity. The addition of MLT to the samples had no effect on targeting, translocation, or signal peptidase activity, nor did it affect the spectral characteristics of the fluorescent translocation intermediates (Alder et al., 2005).

Time-resolved Fluorescence Spectroscopy

Time-resolved fluorescence lifetimes were measured using an ISS model K2 multifrequency phase fluorometer. NBD samples were excited using a 470 nm laser diode. The NBD emission was filtered using a 495 nm cut-on filter. Fluorescein reference standard (Molecular Probes cat # F-1300) dissolved in 0.1 M NaOH was used for the reference, and the reference lifetime was set to 4.05 ns. The concentration of fluorescein was adjusted to have an emission intensity similar to that of the biochemical samples to be investigated. The phase and modulation data were analyzed using Vinci multidimensional fluorescence spectroscopy analysis software. The background-subtracted data were fit to

several different models to determine which model provided the simplest fit while still yielding a low χ^2 value. Typically, the best fit was obtained with two decay components with two discrete exponential fits. The fit of the data to the model was not improved by assuming the samples contained three components with distinguishable lifetimes, nor by using a Lorentzian fit instead of a discrete fit. The relative mole fractions of NBD probes with two different lifetimes was calculated from the preexponential factors.

Biochemical Analysis of Fluorescent Samples

After each fluorescence experiment was completed, the sample radioactivity was measured using a liquid scintillation counter to determine the amount of εNBD-[^{14}C] Lys present. Typically, 400 μL of sample was placed in a 5 mL insert vial. A triton-based scintillation cocktail (4 mL) was added, the vial was vortexed, and the ^{14}C counts per minute (cpm) were measured. The ratio of the net NBD emission intensity in pulses per second (pps) to the number of NBD probes in the sample in cpm was determined and expressed as the pps/cpm ratio.

Alternatively, 400 μL of sample was sedimented through 400 μL of sucrose cushion buffer (0.5 M sucrose/ 100 mM KOAc (pH 7.5)/ 20 mM HEPES (pH 7.5)/ 3.2 mM $Mg(OAc)_2$) for 7 min at 100,000 rpm and 4°C using a TLA 100.2 rotor and a Beckman Optima TL Ultracentrifuge. The supernatant was removed and put into an insert vial as described above. The pellet was

resuspended in 400 μL Buffer A, transferred to an insert vial, and the ^{14}C cpm that remained associated with the ribosome•nascent chain complex were determined as described above.

CHAPTER III

SYNTHESIS OF A SECOND TRANSMEMBRANE SEGMENT REVERSES THE TRANSLOCON GATING MECHANISM

Experimental Design

A homogenous population of fully assembled integration intermediates was prepared by in vitro translation, in the presence of SRP and ER microsomes, of mRNAs that were selectively truncated in the coding region (Fig. 9). There is no stop codon, so normal termination of translation does not occur and the nascent chain remains bound to the ribosome as peptidyl-tRNA (Do et al., 1996; Krieg et al., 1989). A fluorescent probe was incorporated into the nascent chain by performing the translation in the presence of εNBD-Lys-tRNA, a fluorescent-labeled analog of Lys-tRNA that contains a 6-(7-nitrobenz-2-oxa-1,3-diazol-4-yl)aminohexanoyl (NBD) dye covalently attached to the N^{ε}-amino group of the lysyl side chain (Crowley et al., 1994; Crowley et al., 1993). Thus, an NBD-labeled lysine residue was incorporated into the nascent chain at the position of an in-frame lysine codon in the mRNA. Incorporation of the NBD probe into the nascent chain does not interfere with translation or SRP targeting and processing of the nascent chain (Crowley et al., 1993). The location of the fluorescent probe relative to the ribosome and ER membrane is dictated by the location of the incorporated lysine residue and the length of the nascent chain.

Various stages of the integration process can be studied by altering the length of the nascent chain.

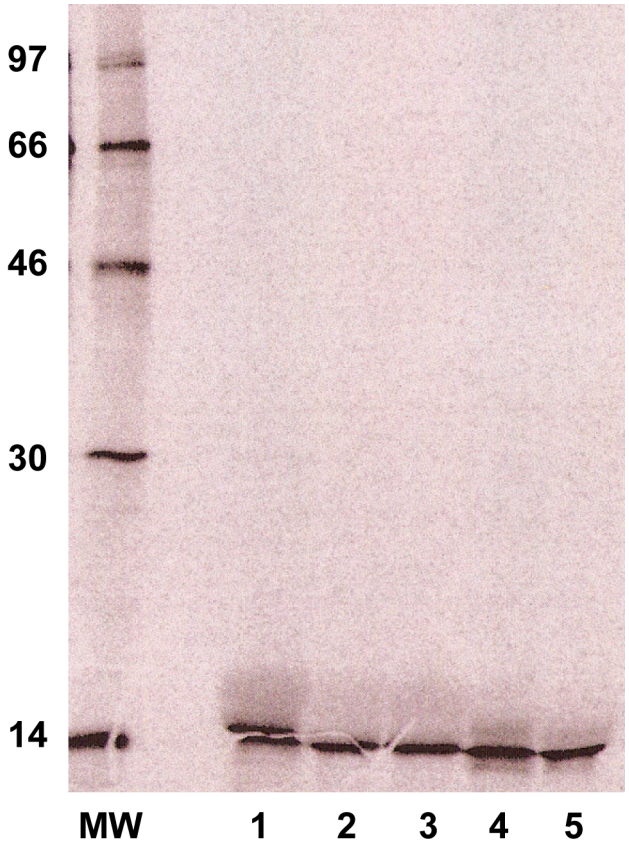

Figure 9. Integration intermediates have a single length of nascent chain.

Various lots of mRNA (mRNA were prepared on different dates and stored at -20°C) were translated in the presence of SRP and ER microsomes to generate integration intermediates having a single length of nascent chain. Lanes 1, 2, and 3 are $2TM_{L53}K2_{171}$. Lanes 4 and 5 are $3TM_{L12,17}K3_{167}$.

Membrane Proteins Used in This Study

Chimeric multi-spanning membrane proteins (MSMP) that contain a single lysine codon were used in this study (Fig. 10). The chimeric proteins 111p and 111+O2p have been well characterized previously (Liao et al., 1997; McCormick et al., 2003), and they served as the templates for the constructs used in this study. All proteins contained a preprolactin (pPL) derived cleavable signal sequence to ensure that the first transmembrane segment (TMS) has type I (N-lumenal/C-cytosolic) orientation. The first TMS is the same as the single TMS from vesicular stomatitus viral G (VSVG) except where noted. The MSMPs also contained one or two additional TMSs from bovine opsin, with varying lengths of nascent chain separating adjacent TMSs. A fragment of the *S. cerevisiae* invertase sequence containing three N-linked glycosylation sites was located immediately after the last TMS, and the remainder of the protein originally came from the proto-oncogene product Bcl-2 (Do et al., 1996).

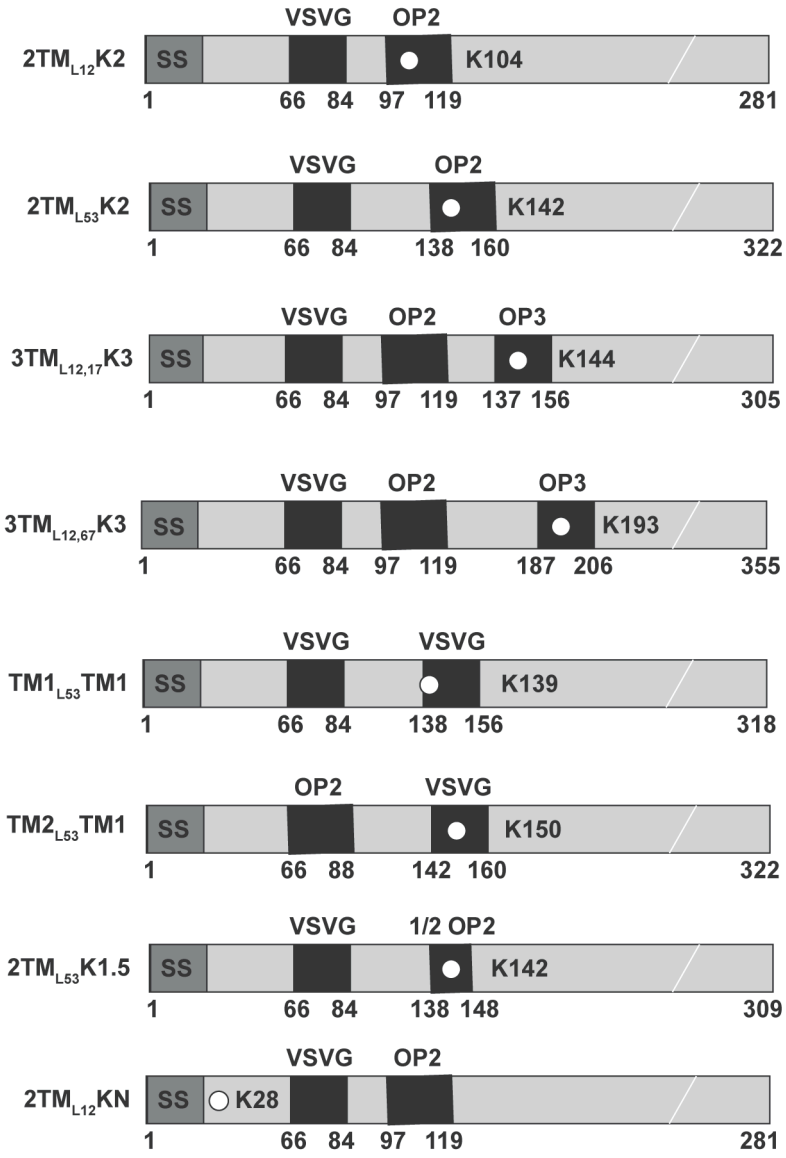

Figure 10. MSMP integration intermediates. The chimeric proteins used in this study are depicted to show the location of the preprolactin-derived signal sequence (SS), the TM domain from vesicular stomatitus G (VSVG), the second and/or third TM domains from opsin (OP2 and OP3, respectively), and the location of the single lysine codon (circle).

The following nomenclature has been used to specify the nascent chain used in an experiment: $2TM_{L12}K2_{122}$, where 2TM denotes the presence of two TMSs (TM1 is VSVG and TMS2 is Opsin2), L12 indicates a 12-residue loop between adjacent TMSs, K2 indicated the lysine codon (and hence probe) is located in TMS2, and 122 is the length of the nascent chain.

In most of the proteins used in this study, the TMSs are oriented in their native orientation after translation and release into the membrane bilayer. However, constructs $TM1_{L53}TM1$ and $TM2_{L53}TM1$ contain TMSs in their non-native orientations. Two identical VSVG TMSs are present in $TM1_{L53}TM1$, so the second TMS is oriented opposite to the native VSVG orientation. The $TM2_{L53}TM1$ contains the second TMS from opsin, followed by the VSVG TMS, so each of these TMSs are oriented opposite to their native orientations in the membrane. Even though the TMSs were not in their native orientation, when these two proteins were translated in the presence of SRP and ER microsomes, both proteins were integrated into the membrane in an N-lumenal/C-cytosol orientation as determined by carbonate extraction and Endo H treatment (Fig. 11).

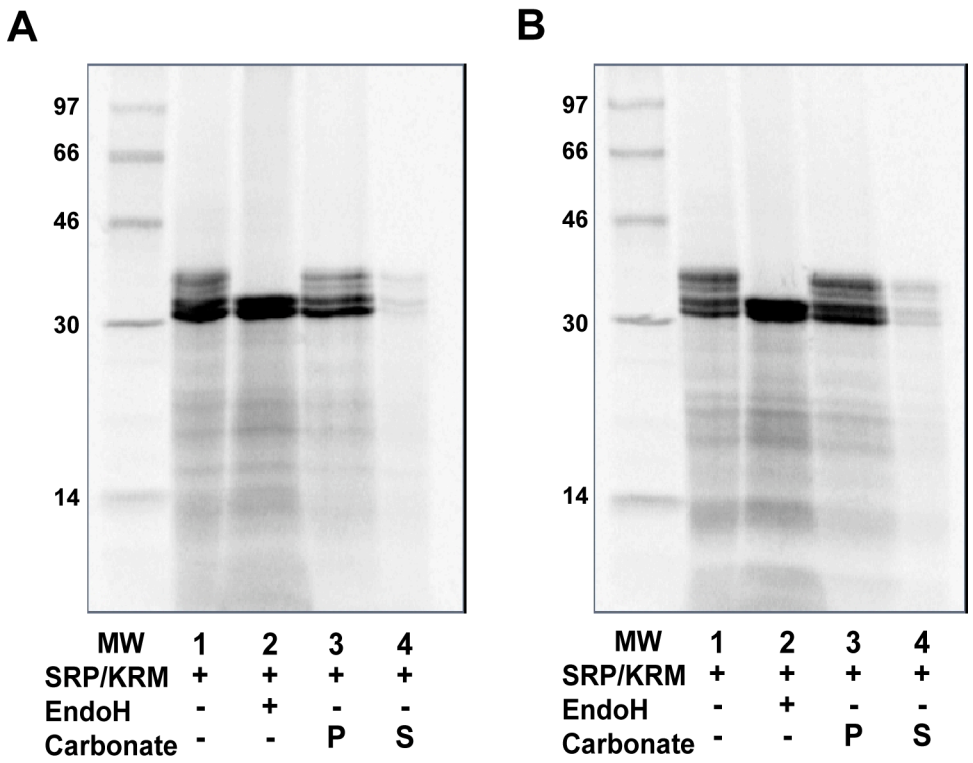

Figure 11. The integration of $TM2_{L53}TM1$ and $TM1_{L53}TM1$.

The integration and orientation of (A) $TM2_{L53}TM1$ and (B) $TM1_{L53}TM1$ in the membrane are shown. Full length mRNA were translated in the presence of SRP and ER microsomes, then processed prior to SDS-PAGE. The proteins are efficiently integrated into the membrane as shown by their insolubility in alkaline buffer (pH 11.5) (compare lanes 3 and 4). The C-termini are located in the lumen as shown by glycosylation of the invertase domain (compare lanes 1 and 2).

Collisional Quenching of NBD

Nascent chain accessibility to the cytosol and the lumen was assessed by measuring the fluorescence emission intensity of NBD in the presence of hydrophilic collisional quenchers. Iodide ions are efficient collisional quenchers of NBD (Crowley et al., 1993) and were used for the experiments presented here. Collisional quenching occurs when a quenching agent, such as an iodide ion, collides with a fluorophore in the excited state, and the excited state energy is lost without emitting a fluorescent photon. The intensity of fluorescence emitted by the sample is therefore reduced by such collisions. The extent of fluorescence quenching is dependent upon the number of collisions, and hence is directly proportional to the concentration of quencher, as described by the Stern-Volmer equation: $(F_0/F) - 1 = K_{sv}$ [Q], where F_0 is the initial net fluorescent intensity, F is the net emission intensity in the presence of the quencher, and [Q] is the concentration of quencher. The Stern-Volmer constant, K_{sv}, is equal to $k_q\tau_0$, where k_q is the bimolecular quenching constant and τ_0 is the lifetime of the fluorophore in the absence of quencher. Graphical analysis using this equation will yield a linear function in which the slope (K_{SV}) is proportional to the extent of quenching. Hence, a larger K_{SV} value is indicative of increased quenching.

The accessibility of the nascent chain to the cytosol was determined by adding iodide ions to the cytosol and directly monitoring the fluorescence intensity of the NBD probe (Fig. 12). If the nascent chain was exposed to the

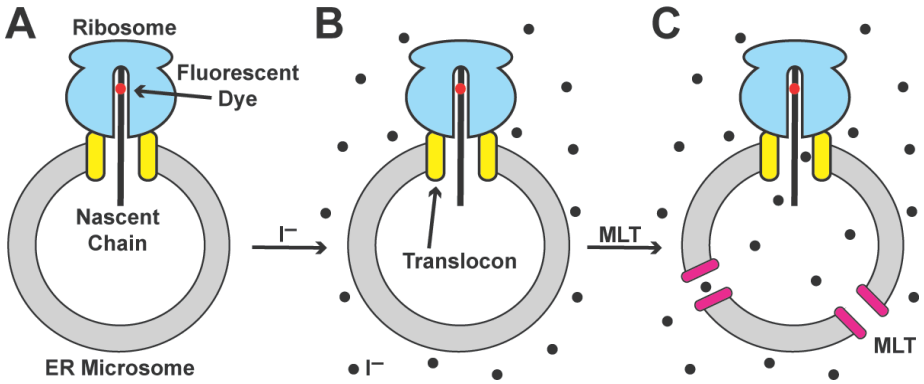

Figure 12. Collisional quenching of fluorescence. (A) The initial fluorescence emission intensity of the probe located in the nascent chain is measured. (B) The emission is monitored after iodide ions are added to the cytosol to assess nascent chain exposure to the cytosol. (C) Iodide ions are introduced into the lumen through MLT-dependent pores formed in the membrane to assess nascent chain exposure to the lumen.

cytosol, a decrease in fluorescence intensity would be observed due to collisional quenching. If a ribosome-translocon junction prevented cytosolic iodide ions from accessing the nascent chain probe (Fig. 12B), collisional quenching would not be observed because iodide ions are not able to penetrate the hydrophobic core of the membrane (Cranney et al., 1983). The inability of cytosolic iodide ions to collisionally quench the fluorescence of the nascent chain probe would infer that the nascent chain was not exposed to the cytosol.

If the cytoplasmic end of the translocon pore is sealed by an ion-tight ribosome-translocon junction, then one would expect the lumenal end of the pore to be open to allow nascent chain entry into the lumen. Nascent chain exposure to the lumen was assessed by introducing iodide ions into the lumen and measuring the fluorescence intensity of the probe (Fig. 12C). The cytolytic peptide Melittin (MLT) was used to create pores in the ER membrane, thereby allowing iodide ions to enter the microsomes (Alder et al., 2005). Lumenal iodide ions restricted to the aqueous phase, yet are able to move through the translocon pore and into the ribosomal tunnel to quench the probe (Alder et al., 2005; Crowley et al., 1994; Haigh and Johnson, 2002; Hamman et al., 1997; Liao et al., 1997). Probes that were not previously quenched because they were not accessible to the cytosol would now be quenched if they were exposed to the aqueous environment of the lumen.

We typically compare the extent of fluorescence quenching observed before and after the addition of MLT. When an ion-tight ribosome-translocon

seal is formed at the cytoplasmic end of the translocon pore, the extent of quenching will differ ± MLT. When the translocon pore is sealed lumenally, the extent of quenching ± MLT is the same. Therefore, the presence or absence of MLT-dependent quenching reveals directly whether or not the ribosome is forming an ion-tight junction with the translocon.

The MLT-induced pore (Fig. 13), having an inner diameter of 25-30 Å (Katsu et al., 1988; Ladokhin et al., 1997), has been described as a barrel-stave model (Naito et al., 2000; Sansom, 1991; Vogel and Jahnig, 1986). MLT peptides, which form an amphiphilic alpha-helix when associated with the membrane (Matsuzaki et al., 1997), aggregate and insert into the lipid bilayer so that the hydrophobic regions align with the lipid core and the hydrophilic peptide regions form the interior of the of the pore (Brogden, 2005). This peptide-induced loss of permeability barrier is believed to be responsible for the cytolytic activity of MLT (Matsuzaki et al., 1997). MLT-induced formation of pores in the lipid bilayer is utilized during the collisional quenching experiments to introduce I^- into the microsomes.

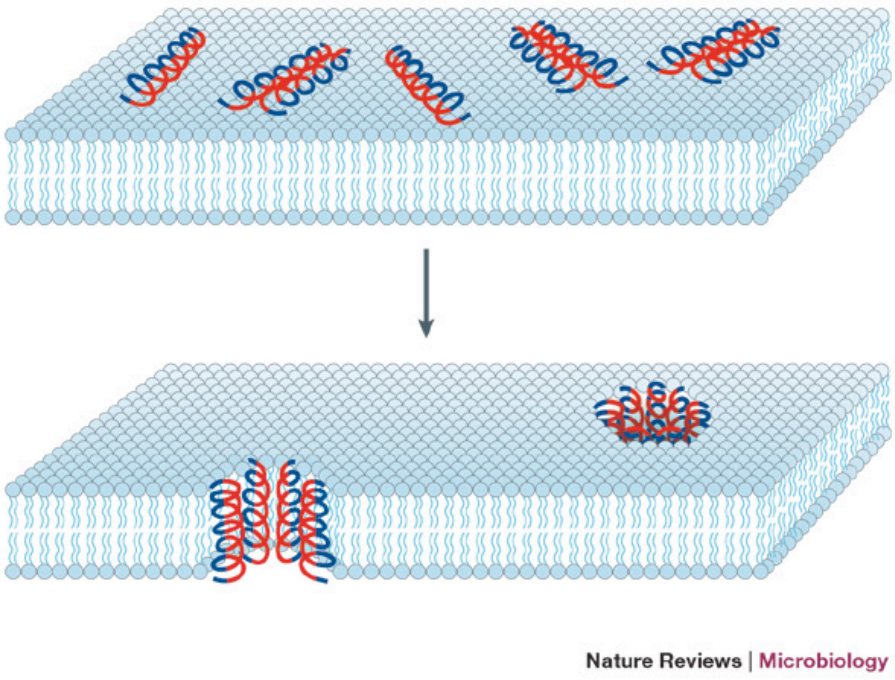

Figure 13. The barrel-stave model of MLT-induced pore formation. Amphiphilic peptides aggregate and insert into the lipid bilayer. The hydrophilic region (red) forms the interior of the pore while the hydrophobic region (blue) associates with the core of the bilayer. Reprinted by permission from Nature Reviews Microbiology: (Brogden, 2005), copyright Macmillan Publishers Ltd 2005.

The Fluorescence Lifetime of NBD Does Not Vary with Respect to Its Location in the Ribosomal Tunnel

A factor that could contribute to observing different K_{SV} values in different collisional quenching experiments is a variation in the lifetime (τ) of the NBD dye caused by differences in the environment of the nascent chain probe. NBD is a water-sensitive fluorophore that has a lifetime of approximately 1 ns in an aqueous milieu and approximately 8 ns in a nonpolar environment (Crowley et al., 1993; Ramachandran et al., 2004). Since the K_{SV} is equal to $k_q\tau$, any change in the lifetime of the NBD dye will have a direct effect on the observed K_{SV}. In order to determine whether such differences occurred, the fluorescence lifetime of NBD incorporated into the second TMS of $2TM_{L12}K2$ (Fig. 10) was measured at different locations in the ribosomal tunnel. The data are shown in Table 3.

The background-subtracted data were fit to several different models to determine which model provided the simplest fit while still yielding a low χ^2 value. Typically the best model contained two decay components with two discrete exponential fits. Assuming the samples contained three components with distinguishable lifetimes did not improve the fit of the data to the model. The relative mole fractions of NBD probes in the two different environments were determined from the preexponential factors. Thus, the best-fit lifetime data indicated the presence of two lifetime components in each sample, the first

Table 3. Fluorescence lifetimes of NBD in MSMPs.

MSMP	τ_1 (ns)	Molar Ratio 1	τ_2 (ns)	Molar Ratio 2	χ^2
$2TM_{L12}K2_{122}$	2.8	0.57	8.9	0.43	12
$2TM_{L12}K2_{130}$	2.7	0.61	9.3	0.39	8
$2TM_{L12}K2_{148}$	2.6	0.59	9.5	0.41	3
$2TM_{L12}K2_{160}$[a]	2.6	0.56	9.4	0.44	7

Samples were prepared as described in Ch. II. The combined fluorescence data from 3 independent experiments were analyzed and fit to a two-component model in which each component was a discrete exponential decay with the indicated lifetime (τ) and molar ratio. χ^2 values were calculated as described previously (Jameson et al., 1984).

[a]Data obtained from two independent experiments.

component having a shorter lifetime synonymous with a more aqueous environment, and the second component having the longer lifetime expected of a more nonpolar environment. This two component lifetime for NBD has previously been observed with nascent secretory proteins (Crowley et al., 1994), nascent membrane proteins (Liao, unpublished data; Lin, unpublished data), and mitochondrial proteins (Alder and Johnson, 2008). εNBD-Lys has a single component lifetime of 1.4 ns in an aqueous buffer (Crowley et al, 1993), but when the dye is incorporated into a nascent chain and purified away from the ribosome and membrane, a two component lifetime, with 80-90% being a short lifetime synonymous with an aqueous environment, is observed (Crowley et al, 1993; Lin, unpublished data). While the origin of the 2-component NBD lifetime is still uncertain, the data in Table 3 indicate that the second component arises when the dye is incorporated into a polypeptide, and hence is a function of being in a protein polymer.

All of the samples yielded similar lifetime values and molar ratios for both the aqueous and the nonpolar components (Table 3). Because there were no significant differences in the average lifetimes of NBD for different lengths of nascent chain, the K_{SV} values observed are believed to be the result of nascent chain exposure to and collisional quenching by iodide ions, not from changes in the nascent chain environment.

Some Nascent Chains with Multiple TMSs Are Not Properly Engaged with the Translocon

Some NBD quenching by cytosolic iodide ions is observed in the absence of MLT for samples containing long nascent chains with multiple TMSs. As a result, these samples have larger "-MLT" quenching than has been observed with secretory proteins (Alder et al., 2005; Crowley et al., 1994; Crowley et al., 1993; Hamman et al., 1997; Hamman et al., 1998). What are some possible explanations for the increased quenching in MSMP samples when compared to secretory proteins?

The observed -MLT quenching most likely originates from a variety of factors including polysome formation (Hamman et al., 1997), adsorption of non-targeted nascent chains to the outside of the membrane (Hamman et al., 1997), and dissociation of properly targeted ribosome•nascent chain complexes (RNCs) from the translocon (Crowley et al., 1994). Each of these effects will expose NBD-labeled nascent chains to the cytosol. If these possibilities are indeed the reasons for the significant –MLT quenching, the residual quenching should be minimized by performing a limited protease and ribonuclease treatment on the samples prior to purification by gel filtration chromatography, as was previously observed when working with pPL (Hamman et al., 1997). Any nascent chains that were not properly targeted to the translocon, but were instead adsorbed to the cytoplasmic surface of the microsome, should be digested by proteinase K (ProK) added to the cytosol. A limited ribonuclease

treatment will degrade any present polysomes to monosomes. The nuclease cleaves mRNA that is not protected from exposure by the ribosome (Wolin and Walter, 1988). RNCs that were properly targeted to the translocon remain bound to the membrane and can now be purified away from those improperly targeted RNCs that are located in the cytoplasm.

When a combination of a limited protease and ribonuclease treatment was performed on samples containing membrane bound RNCs ($2TM_{L53}K2_{171}$, Fig. 10), more than 50% of the –MLT quenching was eliminated. The observed K_{SV} resulting from quenching by cytosolic I^- in the absence of MLT decreased from 2.2 M^{-1} with no protease and ribonuclease treatment to 0.9 M^{-1} after such a treatment (Fig.14 compare A with B, Table 4). This combination of treatments was able to substantially reduce the K_{SV} value observed in the absence of MLT, inferring that the increased –MLT quenching seen when working with long nascent chains containing multiple TMSs is due to the adsorption of improperly targeted nascent chains to the outside of the membrane, polysome formation by translating ribosomes, and the dissociation of properly targeted RNCs from the membrane.

Since exposing a sample to either nuclease or protease carries the risk of damaging the samples, most of my samples were not subjected to a limited protease and nuclease treatment. Instead, I focused on the magnitude of the

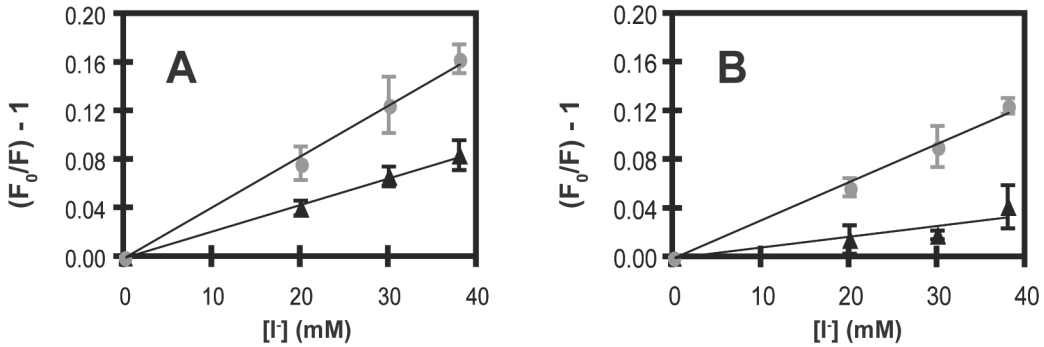

Figure 14. Iodide ion quenching of $2TM_{L53}K2_{171}$ integration intermediates. Samples containing NBD-labeled $2TM_{L53}K2_{171}$ (A) and $2TM_{L53}K2_{171}$ after limited protease and nuclease treatment (B) were prepared and purified as described in Ch II. Iodide ion quenching was assessed using constant-ionic strength procedures. The membrane-bound integration intermediates were examined both before (▲) and after (●) the addition of MLT (5 μM final concentration). The data shown are the average of 3-6 independent experiments.

Table 4. Iodide ion quenching of NBD-labeled MSMP integration intermediates containing two TMSs separated by a long loop.

Membrane Protein	Observed K_{SV} (M^{-1})		ΔK_{SV} (M^{-1})
	-MLT	+MLT	
$2TM_{L53}K2_{163}$	3.1	3.4	0.3
$2TM_{L53}K2_{166}$	1.8	4.0	2.2
$2TM_{L53}K2_{171}$	2.2	4.2	2.0
$2TM_{L53}K2_{171}$ (PK + nuc)	0.9	3.3	2.4

The K_{SV} values shown are the average of 3-6 independent experiments. The standard deviations for the K_{SV} values were $\pm$ 0.1-0.3 M^{-1}. Samples were prepared as described in Ch. II.

difference in quenching (ΔK_{SV}) observed with nascent chain exposure to cytosolic and lumenal iodide ions ($\pm$ MLT). The observed ΔK_{SV} values for treated and untreated samples remained the same within error (Table 4). This approach allowed me to compare the exposure of sample NBDs to I^- in the presence and absence of MLT. Since adding MLT to a sample will only increase the quenching if some dyes are exposed to the lumen instead of the cytosol, the ΔK_{SV} is a measure of the number of nascent chain NBD dyes facing the lumen instead of the cytosol. Thus, when the NBD probes in the nascent chain are exposed to the cytoplasm, the observed ΔK_{SV} will be approximately 0 M^{-1}.

TMS2-dependent Closing and Opening of Opposite Ends of the Translocon Pore

A type I signal-cleaved, single-spanning membrane protein containing a single VSVG TMS was previously studied in detail using fluorescence spectroscopy and photocross-linking (Haigh and Johnson, 2002; Liao et al., 1997). After RNC targeting to the ER microsome was completed, the ribosome formed an ion-tight seal with the translocon (Fig. 6), and the nascent membrane protein was exposed to the lumen (Liao et al., 1997). When the nascent chain increased in length by two additional residues an intermediate state was observed where both cytosolic and lumenal gates were closed, and the nascent chain probe was no longer accessible from either side of the membrane. The ribosome-membrane junction then opened to expose the probe to the cytosol

after the nascent chain had increased in length by several more residues. The closing of the lumenal gate and the opening of the translocon to the cytosol were both effected while the nascent chain length increased by only 5 residues (Liao et al., 1997). The Hsp70 chaperone BiP was required to seal the lumenal end of the translocon pore, either directly or indirectly, in an ATP-dependent reaction (Alder et al., 2005; Haigh and Johnson, 2002). After termination of protein synthesis, the translocon returned back to its ribosome-free state and the membrane protein was fully integrated into the ER membrane. These results suggested that it was the ribosome, not the translocon, that first recognized a TMS and distinguished between nascent secretory and membrane proteins. Clearly, the mechanism by which the permeability barrier of the ER membrane is maintained is very precise because these significant conformational changes occurred while the nascent chain was extended by only 5 residues.

What happens when a second TMS is synthesized and moves into the ribosomal tunnel? Does the ribosomal seal with the translocon re-form after TMS2 enters the tunnel? If yes, will the lumenal end of the then pore re-open to allow egress of the lumenal domain into the ER lumen? To investigate these questions, collisional quenching experiments were performed using a construct previously described in detail (McCormick et al., 2003) containing two TMSs to assess the nascent chain exposure to the cytosol and the lumen at various stages during the co-translational integration of a MSMP into the ER membrane. The fusion protein, designated $2TM_{L12}K2$ (Fig. 10), consists of a pPL derived

cleavable signal sequence, a TMS from VSVG, and the second TMS from bovine opsin, with a 12 residue stretch between the adjacent TMSs (McCormick et al., 2003). Since a single lysine codon is located in the mRNA in TMS2, a single fluorescent probe is incorporated into TMS2 in a nascent chain.

If the ribosomal end of the pore that opened after the synthesis of the first TMS continues to remain open, then cytosolic iodide ions should still be able to access the nascent chain (Fig. 15A), and collisional quenching should be observed. If the ribosome re-engages with the translocon after the synthesis of TMS2 to form an ion-tight seal (Fig. 15B), then the nascent chain will not be exposed to iodide ions located in the cytosol and quenching should not be seen.

When the nascent chain of $2TM_{L12}K2$ was 122 amino acid residues in length, the fluorescence intensity of the probe located in TMS2 was measured before and after the addition of cytosolic iodide ions to determine the "-MLT" K_{SV} (Table 5). At this length, the C-terminal end of TMS2 is located in the ribosomal tunnel only 3 residues away from the peptidyl transferase center (PTC). Since the fluorescence signal was maximally quenched by the externally added

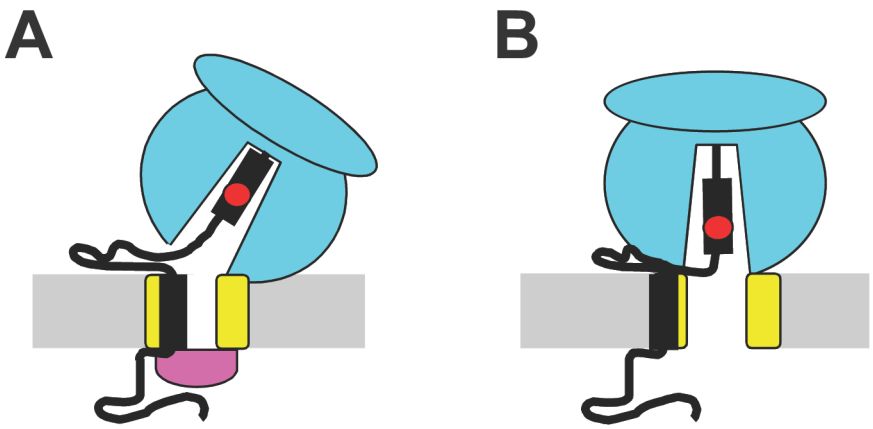

Figure 15. Two possible configurations to maintain the ER membrane permeability barrier during MSMP cotranslational integration. (A) The ribosome (blue) – translocon (yellow) junction at the membrane (grey) is open and BiP (pink) seals the lumenal end of the pore. (B) The ribosome forms an ion-tight seal with the membrane and the lumenal end of the pore is open.

cytosolic iodide ions without adding MLT (Fig. 16A), the nascent chain must be accessible to the cytosol because iodide ions do not penetrate the hydrophobic bilayer (Cranney et al., 1983; Crowley et al., 1994). The data suggest that the ion-tight junction between the ribosome and the translocon that had opened after the synthesis and movement of TMS1 into the ribosomal tunnel (Liao et al., 1997) remains open immediately after the synthesis and movement of TMS2 into the tunnel.

The nascent chain was then extended in length by four additional residues to a total length of 126 amino acids ($2TM_{L12}K2_{126}$), and the NBD fluorescence was again monitored to ascertain the effect of cytosolic iodide ions on NBD intensity. When the C-terminal end of TMS2 was located 7 residues from the PTC, the extent of quenching was not maximal, but was instead approximately equivalent to the nuclease and protease sensitive quenching discussed earlier (p. 61). This quenching, therefore, presumably results from I^- colliding with nascent chains in polysomes or released from the RNC and adsorbed to the microsomal surface. The NBD probes quenched upon addition of MLT must therefore be located within the ribosomal tunnel of an RNC with a tight ribosome-translocon junction, where they can be quenched by lumenal I^-, but not cytosolic I^-. These nascent chains are therefore no longer exposed to

Table 5. Iodide ion quenching of NBD-labeled MSMP integration intermediates containing two TMSs separated by a short loop.

Membrane Protein	Observed K_{SV} (M^{-1})		ΔK_{SV} (M^{-1})
	-MLT	+MLT	
$2TM_{L12}K2_{122}$	2.8	3.2	0.4
$2TM_{L12}K2_{126}$	2.0	4.0	2.0
$2TM_{L12}K2_{130}$	1.9	3.9	2.0
$2TM_{L12}K2_{148}$	1.7	4.2	2.5

The K_{SV} values shown are the average of 3-4 independent experiments. The standard deviations for the K_{SV} values were $\pm$ 0.1-0.3 M^{-1}. Samples were prepared as described in Ch. II.

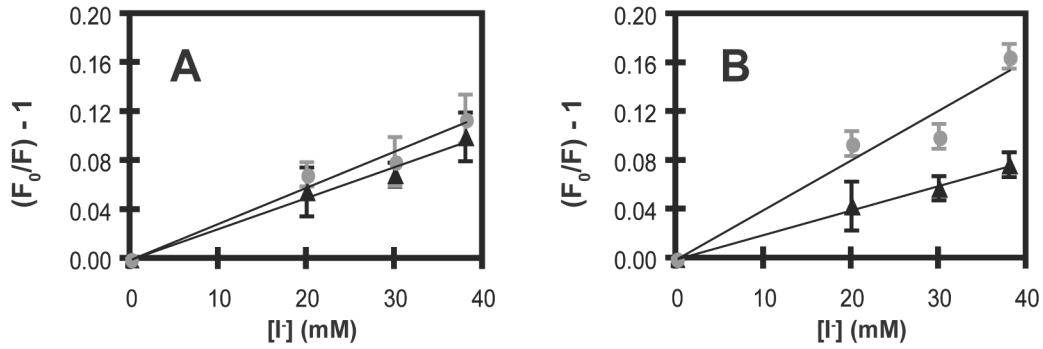

Figure 16. Iodide ion quenching of $2TM_{L12}K2$ integration intermediates. Samples (A) $2TM_{L12}K2_{122}$ and (B) $2TM_{L12}K2_{126}$ were prepared and purified as described in Ch II. Iodide ion quenching was assessed using constant-ionic strength procedures. The membrane-bound integration intermediates were examined both before (▲) and after (⬟) the addition of MLT (5 μM final concentration). The data shown are the average of 3 independent experiments.

the cytosol (Fig. 16B, Table 5). After the addition of MLT formed pores in the ER membrane that allowed iodide ions to be introduced into the lumen, maximum quenching was then observed (Fig. 16B). The MLT-dependent ΔK_{SV} of 2.0 M^{-1} (Table 5) therefore demonstrated that approximately one half of the NBD probes were exposed to the lumen and not the cytosol. (The other half are largely or solely NBDs in nascent chains that are not properly engaged at the translocon, since they are susceptible to removal with protease and/or nuclease.) Since the nascent chain was no longer exposed to the cytosol, the ribosome must have re-formed the ion-tight seal with the translocon. In addition, the lumenal end of the pore must have reopened because lumenal iodide ions were able to move through the translocon and into the ribosomal tunnel to collide with the NBD probe far inside the ribosomal tunnel. The nascent chain then maintained this conformation protected from the cytosol and exposed to the lumen, as the TMS2 probe moved down the tunnel and into the translocon (Table 5, $2TM_{L12}K2_{130}$ and $2TM_{L12}K2_{148}$).

These data suggest that the synthesis and movement of a second TMS into the ribosomal tunnel elicits structural changes with BiP and the ribosome that cause the ribosome to re-form a seal with the translocon and the lumenal gate of the pore to re-open. These changes occur only after TMS2 has moved 4-7 amino acids away from the PTC because collisional quenching by cytosolic iodide ions was observed when the nascent chain was 122 residues in length, but was not observed when the nascent chain was 126 residues long.

This gating sequence is plausible for several reasons. First, it would seem that the lumenal end of the translocon pore would need to be re-opened at some point during the integration process in order to allow the newly synthesized lumenal domain of the MSMP entry into the lumen. Second, the cytosolic end of the translocon would presumably need to be sealed before the lumenal end of the pore was opened to ensure that the integrity of the ER membrane was maintained. Third, increasing nascent chain length by only 5 residues was sufficient to cause the lumenal end of the translocon to close and the ribosomal end to open when the first TMS entered the ribosomal tunnel (Liao et al., 1997). Therefore, it is reasonable that the reversal of the conformational changes when a second TMS enters the ribosomal tunnel also occurs while 4-7 residues are added to the nascent chain. Fourth, the synthesis of a second TMS triggers the re-formation of the ribosome-translocon junction because when only one TMS was present, a nascent chain 130 residues in length remained exposed to the cytosol (Liao et al., 1997). When two TMSs were present, a nascent chain of the same length ($2TML_{12}K2_{130}$) was no longer exposed to the cytosol and was instead accessible to the lumen (Table 5).

The Lumenal End of the Translocon Pore Maintains an Ion-tight Seal When the Cytoplasmic End of the Pore Is Open

So far we have assumed that when the cytosolic end of the pore is open, the lumenal end is sealed to maintain the integrity of the ER membrane. In

order to verify that the lumenal end of the pore is indeed sealed, quenching experiments were performed using a derivative of $2TM_{L12}$ denoted $2TM_{L12}KN$ (Fig. 10). Instead of the fluorescent probe being located in TMS2, the probe was incorporated after the signal sequence at residue 28, which was located in the lumen of membrane-bound RNCs at longer nascent chain lengths. If the lumenal end of the translocon pore were indeed sealed when the cytosolic end is open, the dye located in the lumen should not be exposed to cytosolic iodide ions and no quenching should be observed. After the addition of MLT to induce pore formation in the membrane, iodide ions would then be able to enter the lumen and collisionally quench the emission of the probe. Since we have just shown that the ribosome-translocon junction is breached when $2TM_{L12}K2$ is 122 residues long (Fig.16A), we will use a nascent chain length of 122 to determine whether the lumenal end of the pore is closed.

When iodide ions were added to the cytosol of an $2TM_{L12}KN_{122}$, the fluorescence of the dye located in the lumen was not quenched by the ions (Fig. 17). But, after MLT-induced pore formation in the membrane, the dye located in

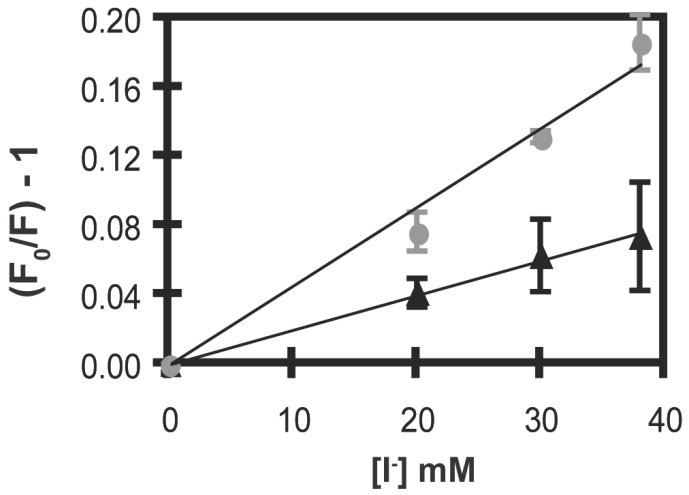

Figure 17. Iodide ion quenching of a nascent chain probe in the lumen, $2TM_{L12}KN_{122}$ integration intermediate. The integration intermediate $2TM_{L12}KN_{122}$, containing a single lysine codon at residue 28 of the nascent chain, was prepared and purified as described in Ch. II. Iodide ion quenching was assessed using constant-ionic strength procedures. The membrane-bound integration intermediates were examined both before (▲) and after (●) the addition of MLT (5 μM final concentration). The data shown are the average of 2 independent experiments.

the lumen was quenched, giving a ΔK_{SV} of 2.6 M^{-1} (Fig. 17). Since the nascent chain probe inside the ribosome is quenched by cytosolic I^- in $2TM_{L12}K2_{122}$ (Fig. 16A), the cytosolic end of the pore is open. Iodide ions are therefore prevented from moving into the lumen by BiP-mediated closure of the lumenal end of the pore and/or a BiP-dependent constriction of the diameter of the aqueous translocon pore. Thus, the lumenal end of the translocon pore is indeed closed when the cytosolic end is open, thereby maintaining the permeability barrier of the membrane.

Cytosolic Pore Closure Occurs Irrespective of TMS Location in the Nascent Chain

Since cytosolic pore closure is effected by a second TMS moving down the ribosomal tunnel, what effect does the length of nascent chain adjoining two TMSs have on pore closure? Will a longer nascent chain loop separating TMS1 and TMS2 interfere with the ribosome's ability to close the cytosolic end of the translocon pore? When the TMSs were separated by a short loop, the seal between the ribosome and the translocon remained open immediately after the synthesis and movement of TMS2 down the tunnel (Table 5, $2TM_{L12}K2_{122}$). One explanation for this may be that a separation of only 12 amino acids does not allow adequate time for the changes to occur at the translocon. By extending the loop separating the TMSs, the ribosome and translocon will have more time to initiate and complete any conformational changes that are required.

To assess the effect of nascent chain loop length on pore opening/closing, the collisional quenching experiments that were performed using $2TM_{L12}K2$ were repeated using $2TM_{L53}K2$ (Figure 10). The two proteins differ only in the number of residues separating the adjacent TMSs; $2TM_{L53}K2$ contains a nascent chain loop that is 53 residues long instead of the shorter, 12-residue loop in $2TM_{L12}K2$. In order to provide the most direct comparison between the two constructs, we chose to focus on three different nascent chain lengths in which the C-terminal end of TMS2 was located in the ribosomal tunnel 3 ($2TM_{L53}K2_{163}$), 6 ($2TM_{L53}K2_{166}$), or 11 ($2TM_{L53}K2_{171}$) residues from the PTC.

When quenching experiments were performed using $2TM_{L53}K2_{163}$ (Fig. 18A), the nascent chain was exposed to the cytosol since maximal quenching was observed with cytosolic iodide ions and the ΔK_{SV} was very low (0.3 M^{-1}, Table 4). An equivalent result was obtained with $2TM_{L12}K2_{122}$ in that the probe in this RNC was also exposed to the cytosol.

When the NBD fluorescence of $2TM_{L53}K2_{166}$ was monitored in the presence of I^- both before and after the addition of melittin, the nascent chain was now found to be exposed to the lumen, not the cytosol (Fig. 18B). The observed ΔK_{SV} of 2.2 M^{-1} (Table 4) shows that maximal collisional quenching was not observed until after MLT-dependent pore formation in the microsomal membrane allowed the quencher entry into the lumen. Similar results were obtained when the nascent chain was extended in length by an additional 5 residues (Table 4, $2TM_{L53}K2_{171}$). These results were comparable to those

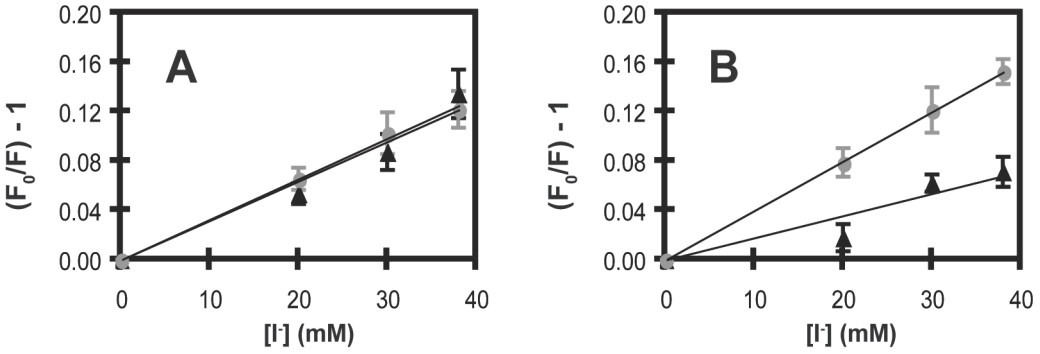

Figure 18. Iodide ion quenching of long-loop integration intermediates. Samples (A) $2TM_{L53}K2_{163}$ and (B) $2TM_{L53}K2_{166}$ were prepared and purified as described in Ch. II. Iodide ion quenching was assessed using constant-ionic strength procedures. The membrane-bound integration intermediates were examined both before (▲) and after (⬟) the addition of MLT (5 μM final concentration). The data shown are the average of 3-4 independent experiments.

obtained with corresponding short loop nascent chains (Table 5, $2TM_{L12}K2_{126}$ and $2TM_{L12}K2_{130}$) in terms of the nascent chain length dependence of the re-establishment of the tight ribosome-translocon junction. Thus, despite the additional length of nascent chain in the cytoplasmic domain of $2TM_{L53}K2$, the ion-tight seal formed by the ribosome at the cytoplasmic side of the translocon pore is still formed only after the C-terminal end of TMS2 moves 4-7 residues from the PTC.

Thus, several conclusions can be drawn. First, the ribosome is able to form and maintain an ion-tight seal with the translocon even after a large cytoplasmic domain of the nascent chain has been synthesized. The details of how the seal is maintained when a nascent chain strand extends into the cytosol are not known at this time. Second, it is the presence of a second TMS, not the length of nascent chain, that elicits pore opening and closing. Third, the ribosome recognizes a TMS and initiates pore closing at the cytosolic and pore opening at the lumenal end when the TMS is located only 4-7 residues away from the PTC.

CHAPTER IV

SEQUENTIAL TRANSMEMBRANE SEGMENTS EFFECT OPPOSITE CHANGES AT THE ER MEMBRANE

Does the Translocon Pore Alternately Open and Close During MSMP Integration?

When the first TMS moves into the ribosomal tunnel, structural changes are initiated at the membrane that result in the closure of the lumenal end and the opening of the cytosolic end of the translocon pore, presumably to allow the cytoplasmic domain of the nascent protein entry into the cytosol (Liao et al., 1997). When the second TMS moves into the ribosomal tunnel, this gating mechanism is reversed to close the cytosolic end and open the lumenal end of the pore. Does the synthesis and movement of a third TMS down the ribosomal tunnel trigger another reversal of pore closure (i.e., close the lumenal end and open the cytosolic end), just as was seen with TMS1? In other words, does the translocon pore alternately open and close as sequential TMSs of a MSMP are co-translationally integrated into the bilayer of the ER membrane, thereby directing the newly synthesized lumenal and cytosolic domains of the protein entry into their respective locations?

The Ribosome-Translocon Junction Is Re-opened by a Third TMS

To determine the effect of a third TMS, a construct, $3TM_{L12,17}K3$ (Fig. 10), containing the third TMS from opsin, located 17 amino acids downstream from TMS2, and a single lysine codon in TMS3. Collisional quenching was then used to examine integration intermediates with nascent chains truncated 3, 6, or 11 residues from the C-terminal end of TMS3, the same truncation sites used in the previous TMS1 and TMS2 investigations.

We first looked at the state of the translocon when TMS3 was located 3 residues from the PTC, having a nascent chain length of 159 amino acids residues. Studies of TMS1 (Liao et al., 1997) and TMS2 (Ch. III) revealed that pore opening/closing occurs after a TMS has moved 4-7 residues from the PTC. If this pattern were to be repeated with TMS3, we would expect to see that the ribosome is still engaged with the translocon when TMS3 is located only 3 residues from the PTC, and that the nascent chain would only be accessible to lumenal iodide ions after the addition of MLT. When I^- was added to the cytosol, the fluorescence intensity of the probe located in TMS3 was not maximally quenched, therefore indicating that the nascent chain is not exposed to the cytosol in this integration intermediate (Fig. 19A, Table 6). After the quencher was introduced into the lumen through MLT-induced pores, the nascent chain was exposed to the lumen and the NBD fluorescence was quenched, yielding a ΔK_{SV} of 2.3 M^{-1} (Table 6). Thus, the conformational changes at the membrane

that were effected during the passage of TMS2 through the ribosomal tunnel remained in effect immediately after the synthesis of TMS3.

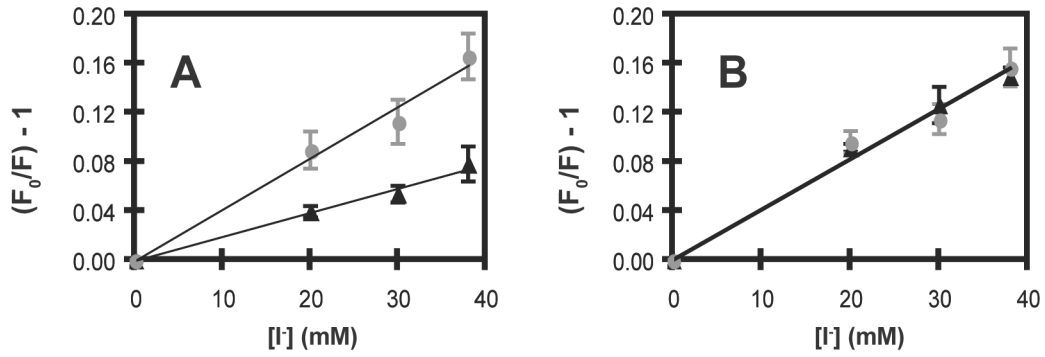

Figure 19. Iodide ion quenching of integration intermediates containing 3 TMSs. Samples (A) $3TM_{L12,17}K3_{159}$ and (B) $3TM_{L12,17}K3_{162}$ were prepared and purified as described in Ch. II. Iodide ion quenching was assessed using constant-ionic strength procedures. The membrane-bound integration intermediates were examined both before (▲) and after (●) the addition of MLT (5 μM final concentration). The data shown are the average of 3-4 independent experiments.

Table 6. Iodide ion quenching of NBD-labeled MSMP integration intermediates containing three TMSs.

Membrane Protein	Observed K_{SV} (M^{-1})		ΔK_{SV} (M^{-1})
	-MLT	+MLT	
$3TM_{L12,17}K3_{159}$	1.9	4.2[a]	2.3
$3TM_{L12,17}K3_{162}$	4.1	4.1	0.0
$3TM_{L12,17}K3_{167}$	4.2[a]	4.4	0.2
$3TM_{L12,67}K3_{209}$	2.0	4.1	2.1
$3TM_{L12,67}K3_{212}$	3.9	4.1	0.2

The K_{SV} values shown are the average of 3-4 independent experiments. The standard deviations for the K_{SV} values were $\pm$ 0.1-0.2 M^{-1} except where indicated. Samples were prepared as described in Ch. II.
[a]The standard deviations were $\pm$ 0.3 M^{-1}.

In contrast, when quenching experiments were performed with $3TM_{L12,17}K3_{162}$ (Fig. 19B), we found that cytosolic iodide ions were able to access the nascent chain and maximally quench the fluorescence (Table 6). In order for the nascent chain to be exposed to the cytosol, the ribosome-translocon junction must have re-opened because the probe was still located far inside the ribosome tunnel and was not exposed to the cytosol when the nascent chain was 159 residues long. The nascent chain also remained exposed to the cytosol as translation continued (Table 6, $3TM_{L12,17}K3_{167}$).

Movement of TMS1 into the ribosomal tunnel effected closure of the lumenal end of the pore and also opened its cytosolic end (Liao et al., 1997). The entry of TMS2 into the tunnel reversed the gating of the pore by opening the lumenal end and re-forming the ribosome-translocon junction. TMS3 initiated the same changes at the membrane as TMS1. Thus, the pore appears to be alternately closed by lumenal BiP and the cytoplasmic ribosome as TMSs having opposite orientations are cotranslationally moved through the ribosomal tunnel and integrated into the ER membrane.

A Longer Nascent Chain Loop Between Adjoining TMSs Only Delays When TMS3-Dependent Changes Occur at the Membrane

To determine what effect increasing the length of polypeptide between TMS2 and TMS3 would have on structural changes at the membrane, we repeated the collisional quenching experiments using construct $3TM_{L12,67}K3$

(Figure 10), that contains a 67-residue loop between TMS2 and TMS3 instead of a 17-residue loop.

When the C-terminal end of TMS3 was 3 amino acids from the PTC, the addition of iodide ions to a sample containing $3TM_{L12,67}K3_{209}$ integration intermediates did not yield maximal quenching (Fig. 20A). Since the quenching was maximal only after the addition of MLT (Fig. 20A, Table 6), the NBD dyes and nascent chains that were properly engaged at the membrane were exposed to the lumen, not the cytosol. Thus, even though TMS3 had been completely synthesized and was present in the ribosomal nascent chain tunnel, no changes had occurred at the membrane. However, after an additional 3 amino acid residues were synthesized ($3TM_{L12,67}K3_{212}$, Fig. 20B), the nascent chain was maximally quenched by $^{I-}$ and hence accessible to the cytosol, as shown by the very low ΔK_{SV} of 0.2 M^{-1} (Table 6).

Thus, the longer loop between TMS2 and TMS3 only delayed the time at which changes occurred at the membrane. These changes were triggered, as with TMS1 and TMS2, by TMS3 moving into the ribosomal tunnel. In fact, since changes occur at the membrane only after the C-terminal end of a TMS (TMS1, TMS2, TMS3) moves 4-7 residues from the PTC, it is clear that the important polypeptide distance is that between the PTC and the TMS, not that between

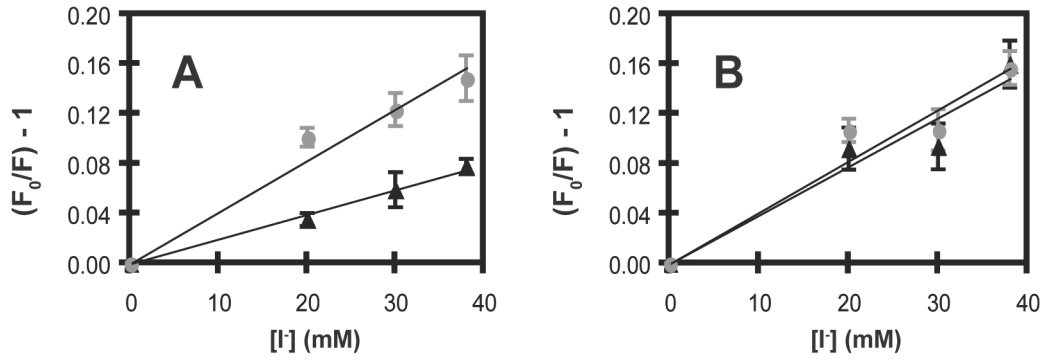

Figure 20. Iodide ion quenching of integration intermediates with a longer TMS2-TMS3 loop. Samples (A) $3TM_{L12,67}K3_{209}$ and (B) $3TM_{L12,67}K3_{212}$ were prepared and purified as described in CHAPTER II. Iodide ion quenching was assessed using constant-ionic strength procedures. The membrane-bound integration intermediates were examined both before (▲) and after (●) the addition of MLT (5 μM final concentration). The data shown are the average of 3 independent experiments.

TMSs. The length of the loop between adjacent TMSs does not appear to affect the ribosome's ability to recognize a TMS or to initiate conformational changes at the membrane.

The ribosome therefore recognizes each TMS soon after it is synthesized and moves into the ribosomal tunnel. The passage of each TMS in turn elicits a response that results in the alternate opening and closing of each end of the aqueous translocon pore as the sequential TMSs of a MSMP are cotranslationally integrated into the nonpolar core of the bilayer (Fig. 21). By ensuring that one end of the translocon pore remains closed at any given time during translation, the membrane is able to maintain its integrity and minimize ion leakage from the lumen into the cytosol.

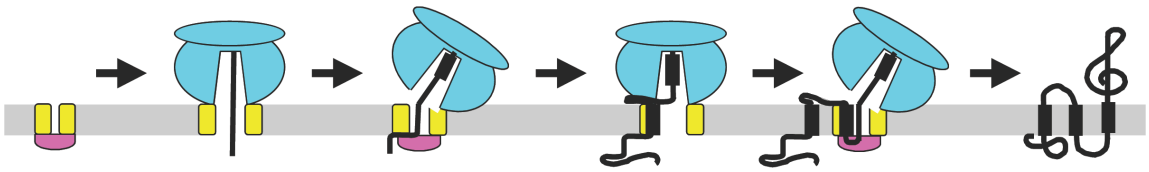

Figure 21. Cotranslational integration of a MSMP into the ER membrane.

The translocon pore is alternately opened and closed as each sequential TMS of a MSMP is synthesized and moves down the ribosomal tunnel into the translocon.

CHAPTER V

TRANSLOCON PORE OPENING AND CLOSING IS TMS DEPENDENT

One Half of a TMS Is Not Sufficient to Elicit Changes at the Membrane

The data presented in the previous chapter demonstrate that the critical structural feature for eliciting pore opening and closing is the presence of a TMS. It therefore is appropriate to characterize further what structural features of the TMS are recognized.

When quenching experiments were performed using a single-spanning membrane protein that contained only the 10 N-terminal residues of the VSVG TMS (TMS1), no quenching by cytosolic iodide ions was observed (Liao et al., 1997). The ribosome was therefore able to distinguish between a complete TMS and a partial TMS in regulating translocon gating. To determine whether the ribosome recognizes TMS2 in the same manner as TMS1, a fusion protein identical to $2TM_{L53}K2$ was prepared, except that the terminal 13 residues of opsin TMS2 were deleted (Fig. 10). This protein was designated $2TM_{L53}K1.5$. A biochemical analysis of full length $2TM_{L53}K1.5$ showed that the ribosome did not recognize the remaining 10 amino acids as an intact TMS (Fig. 22). TMS1 was

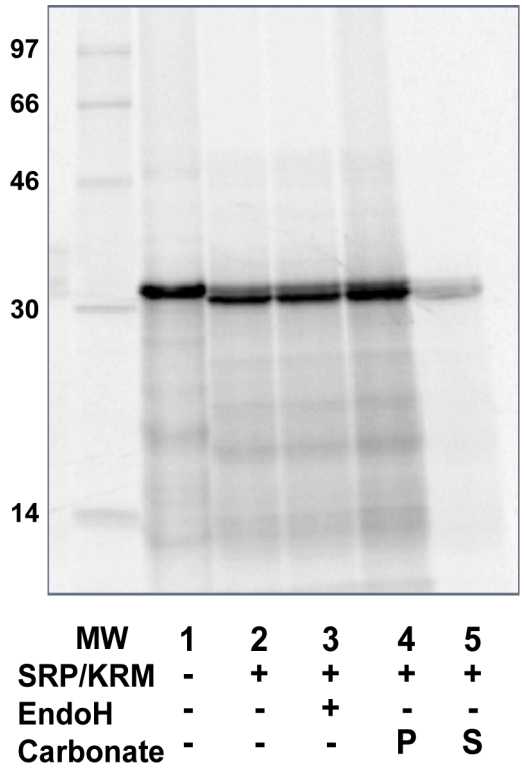

Figure 22. The integration of $2TM_{L53}K1.5$. The integration and orientation of $2TM_{L53}K1.5$ in the membrane is shown. Full length mRNA were translated in the presence or absence of SRP and ER microsomes, then processed prior to SDS-PAGE. The protein is efficiently integrated into the membrane as shown by its insolubility in alkaline buffer (pH 11.5) (compare lanes 4 and 5). It has an N_{lum}-C_{cyt} orientation as shown by signal cleavage of the N-terminus (lane 2). The C-terminus is located in the cytosol because there is no glycosylation of the invertase domain (compare lanes 2 and 3).

integrated into the bilayer in an N_{lum}-C_{cyt} orientation, as expected. If the partial TMS2 was recognized as a complete TMS and integrated into the membrane, one would expect to see glycoslyation of the invertase domain. No glycoslyation of the invertase domain was observed (compare lanes 2 and 3). Thus, the partial TMS was not integrated into the membrane.

The quencher-dependent emission intensity of NBD was monitored for nascent chain lengths of 163 and 171 amino acids using integration intermediates of $2TM_{L53}K1.5$. Cytosolic iodide ions maximally quenched the NBD fluorescence at both lengths (Table 7), thereby indicating that the nascent chain is exposed to the cytosol when the nascent chain is 163 residues long (Fig. 23A) and remains exposed to the cytosol as translation continues (Fig. 23B). These results differ from those observed with a complete TMS2. Since the ribosome-translocon junction was re-formed with $2TM_{L53}K2_{171}$, but not with $2TM_{L53}K1.5_{171}$, it appears that the ribosome is capable of differentiating between hydrophobic stretches of nascent chain that are 10 or 23 residues long. Furthermore, one half of a TMS is not sufficient to elicit the structural changes to change the gating at the membrane. Thus, ribosome recognition of a TMS requires a certain number of nonpolar residues in sequence (this has not been determined), and this is true for both the first and second TMSs through the tunnel.

Table 7. Iodide ion quenching of NBD-labeled MSMP integration intermediates that contain an incomplete TMS.

Membrane Protein	Observed K_{SV} (M^{-1})		ΔK_{SV} (M^{-1})
	-MLT	+MLT	
$2TM_{L53}K1.5_{163}$	3.4	3.6	0.2
$2TM_{L53}K1.5_{171}$	3.6	3.8	0.2

The K_{SV} values shown are the average of 2 independent experiments. The errors for the K_{SV} values were $\pm$ 0.0-0.3 M^{-1}. Samples were prepared as described in Ch. II.

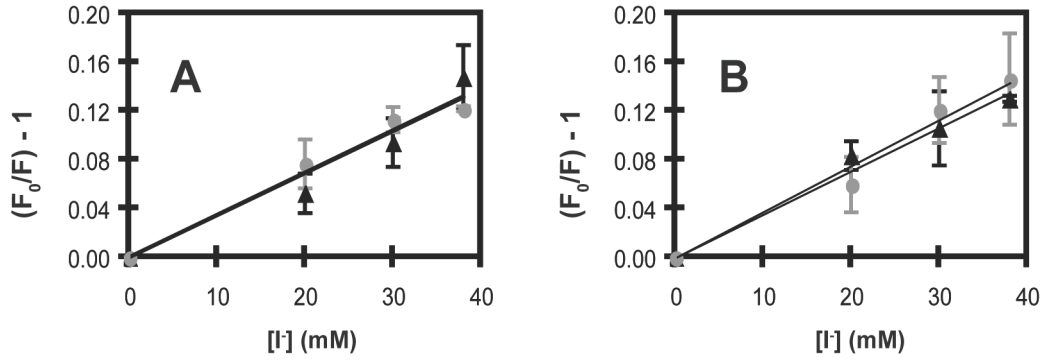

Figure 23. Iodide ion quenching of integration intermediates containing a nascent chain with a truncated TMS. Samples (A) $2TM_{L53}K1.5_{163}$ and (B) $2TM_{L53}K1.5_{171}$ were prepared and purified as described in Ch. II. Iodide ion quenching was assessed using constant-ionic strength procedures. The membrane-bound integration intermediates were examined both before (▲) and after (⬟) the addition of MLT (5 μM final concentration). The data shown are the average of 2 independent experiments.

TMS Recognition by the Ribosome Is Independent of Native Orientation in the Bilayer

In our membrane protein chimera, each TMS is inserted into the bilayer in the same orientation (N_{cyto} or N_{lum}) as in the native proteins from which the TMSs originate. To determine if the ribosome can recognize the native orientation of a TMS to determine how it gates the pore, the order of the TMSs in $2TM_{L53}K2$ was reversed to create a new chimeric protein, $TM2_{L53}TM1$, where the first TMS is TMS2 from opsin and the second TMS is the single TMS in the VSVG protein (Fig. 10). Even though the TMSs were not in their native orientation when $TM2_{L53}TM1$ was translated in the presence of SRP and ER microsomes, the protein was integrated into the membrane in an N-lumenal/C-cytosol orientation as determined by carbonate extraction and protease protection (Fig. 11). Thus, the inversion of the TMSs did not alter the integration detected biochemically.

Does the movement of the first TMS through the ribosomal tunnel elicit ribosome-translocon junction opening as was observed previously (Liao et al., 1997)? By monitoring the emission intensity of a probe positioned in the first TMS of $TM2_{L53}TM1_{91}$, we found that the nascent chain was initially protected from cytosolic I^- and exposed to lumenal I^- (Fig. 24A, Table 8). After the C-terminal end of the TMS moved 6 residues away from the PTC ($TM2_{L53}TM1_{94}$), fluorescence measurements showed that a change in the gating of the translocon had taken place since the nascent chain probe was no longer

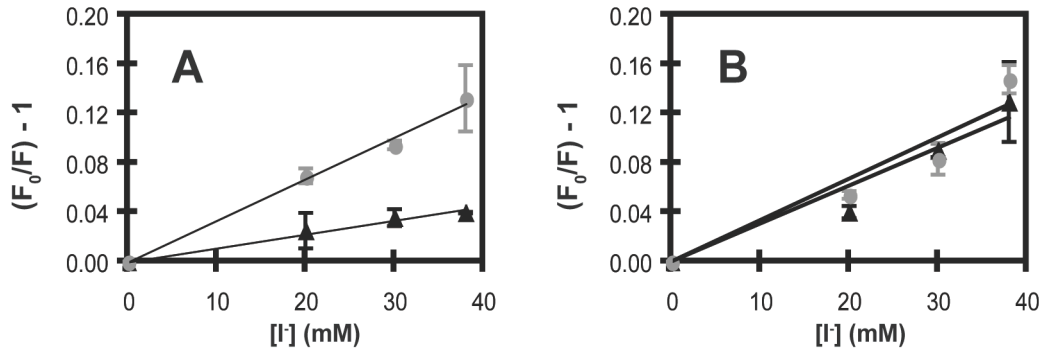

Figure 24. Iodide ion quenching of integration intermediates with TMSs in non-native orientations (part 1). Samples (A) $TM2_{L53}TM1K1_{91}$ and (B) $TM2_{L53}TM1K1_{94}$ were prepared and purified as described in Ch. II. Iodide ion quenching was assessed using constant-ionic strength procedures. The membrane-bound integration intermediates were examined both before (▲) and after (●) the addition of MLT (5 μM final concentration). The data shown are the average of 2 independent experiments.

Table 8. Iodide ion quenching of NBD-labeled MSMP integration intermediates having inverted TMSs.

Membrane Protein	Observed K_{SV} (M^{-1})		ΔK_{SV} (M^{-1})
	-MLT	+MLT	
$TM2_{L53}TM1_{91}$	1.1	3.4[a]	2.3
$TM2_{L53}TM1_{94}$	3.1[a]	3.4	0.3
$TM2_{L53}TM1_{163}$	4.0	4.0	0.0
$TM2_{L53}TM1_{166}$	1.9	4.2	2.3

The K_{SV} values shown are the average of 2 independent experiments. The errors for the K_{SV} values were $\pm$ 0.0-0.2 M^{-1} except where indicated. Samples were prepared as described in Ch. II.
[a]The standard deviations were $\pm$ 0.3-0.4 M^{-1}.

protected from cytosolic I^- (Fig. 24B, Table 8). Thus, the synthesis and movement of the first TMS resulted in closing the lumenal end and opening the cytosolic end of the pore, thereby showing that the native orientation of the TMS is not recognized by the ribosome.

Does the entry of a second TMS into the ribosomal tunnel reverse the structural changes elicited by the first TMS, no matter what the native orientation of the second TMS? After the second TMS was synthesized and located 3 residues from the PTC ($TM2_{L53}TM1_{163}$, Fig. 25A), the ribosome-translocon junction was still open because quenching by cytosolic I^- was maximal before the addition of MLT (Table 8). After the second TMS had moved 6 residues from the PTC ($TM2_{L53}TM1_{166}$, Fig. 25B), cytosolic I^- no longer gave maximal quenching and the ΔK_{SV} was 2.3 M^{-1} (Table 8). Thus, the ion-tight ribosome-translocon junction had reformed and properly-engaged nascent chains were no longer exposed to the cytosol.

Since reversing the orientation of the VSVG TMS and the TMS2 from opsin did not detectably affect the ribosome's ability to recognize these TMSs, and indicate the appropriate structural changes at the membrane, it appears that the ribosome does not distinguish between TMSs based on their orientation in the bilayer. Instead, the ribosome appears to treat each sufficiently-long stretch of nonpolar residues as a TMS and will alternate – by some as-yet undiscovered mechanism – gating of the translocon pore.

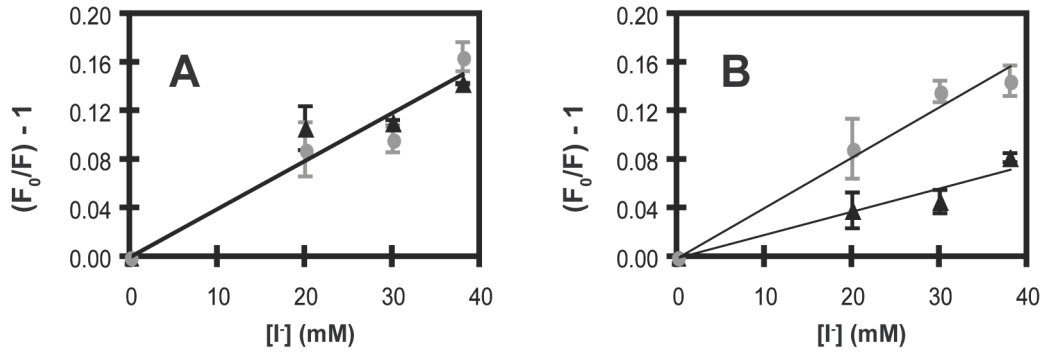

Figure 25. Iodide ion quenching of integration intermediates with TMSs in non-native orientations (part 2). Samples (A) $TM2_{L53}TM1K2_{163}$ and (B) $TM2_{L53}TM1K2_{166}$ were prepared and purified as described in Ch. II. Iodide ion quenching was assessed using constant-ionic strength procedures. The membrane-bound integration intermediates were examined both before (▲) and after (●) the addition of MLT (5 μM final concentration). The data shown are the average of 2 independent experiments.

The Ribosome Recognizes and Elicits a Different Response When Two Identical TMSs Are in a Series

The entry of a single VSVG TMS into the ribosomal tunnel effected changes at the membrane in which the lumenal end of the translocon pore closed and the cytosolic end opened (Liao et al., 1997). If the single TMS from VSVG entered the tunnel a second time, in sequential order, would the ribosome distinguish between the two identical TMSs? If yes, does the ribosome treat the identical TMSs as if they are two unique sequences by eliciting different responses at the membrane as each sequential TMS enters the ribosomal tunnel?

A chimeric protein, designated $TM1_{L53}TM1$ (Fig. 10), was created by replacing TMS2 from opsin in $2TM_{L53}K2$ with the single TMS from VSVG. Thus, the protein contains two VSVG TMSs; the first VSVG TMS maintaining its native orientation (N_{lum}/C_{cyt}) and the second VSVG TMS being inverted. When $TM1_{L53}TM1$ was translated in the presence of SRP and ER microsomes, the protein was integrated into the membrane in an N-lumenal/C-cytosol orientation as determined by carbonate extraction and Endo H treatment (Fig. 11). A single fluorescent probe was incorporated into the second TMS.

Collisional quenching experiments were performed using the $TM1_{L53}TM1$ protein to address the aforementioned questions. If the ribosome does indeed distinguish between and treat identical TMSs as if they are two unique TMSs, then the ribosome-translocon junction would be expected to re-form after the

second TMS entered the tunnel and moved at least 4 residues from the PTC, based on the results obtained during the study of $2TM_{L53}K2$ (Ch. III).

The emission intensity of $TM1_{L53}TM1$ integration samples were monitored when the C-terminal end of the second TMS was located 3 residues from the PTC ($TM1_{L53}TM1_{159}$), and maximal quenching by cytosolic I^- was observed as represented by the low ΔK_{SV} of 0.1 M^{-1} (Fig. 26A, Table 9). The data suggest that the seal between the ribosome and the translocon that was breached after the first VSVG TMS moved through the tunnel remains so upon entry of the second VSVG TMS into the tunnel. However, after the second TMS moved an additional 3 residues down the tunnel ($TM1_{L53}TM1_{162}$), so the TMS was now 6 residues from the PTC, maximal quenching by cytosolic I^- was not observed. Thus, the nascent chain was no longer exposed to cytosol (Fig. 26B). The microsomes were then permeabilized by the addition of MLT, allowing the introduction of I^- into the lumen, and maximal quenching was observed as represented by the ΔK_{SV} of 2.1 M^{-1} (Table 9). Therefore, a change in gating must have taken place since the nascent chain is now protected from the cytosol.

The ribosome does indeed seem to recognize and differentiate between two sequential VSVG TMSs, and the TMSs were treated as if they were two unique sequences because the entry of each TMS into the ribosomal tunnel generated a different response at the membrane. When the first TMS moved

Table 9. Iodide ion quenching of NBD-labeled MSMP integration intermediates having identical TMSs.

Membrane Protein	Observed K_{SV} (M^{-1})		ΔK_{SV} (M^{-1})
	-MLT	+MLT	
$TM1_{L53}TM1_{159}$	4.0	4.1	0.1
$TM1_{L53}TM1_{162}$	2.0	4.1	2.1

The K_{SV} values shown are the average of 2 independent experiments. The errors for the K_{SV} values were $\pm$ 0.0-0.2 M^{-1}. Samples were prepared as described in Ch. II.

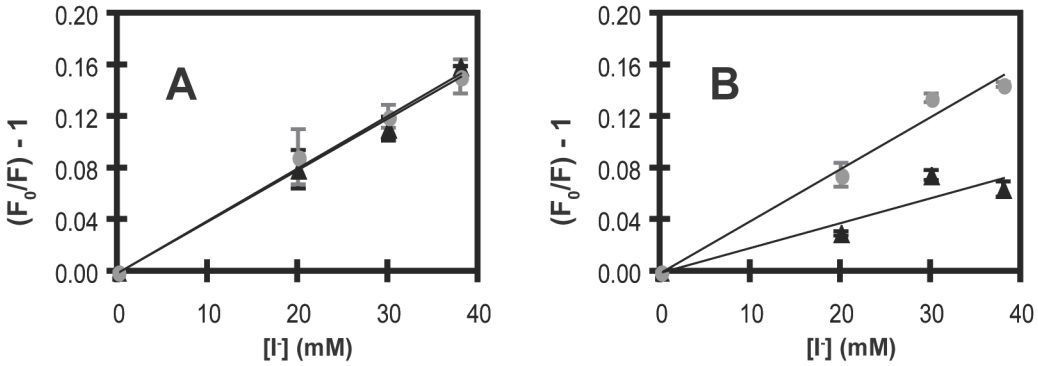

Figure 26. Iodide ion quenching of $TM1_{L53}TM1K2$ integration intermediates. Samples (A) $TM1_{L53}TM1K2_{159}$ and (B) $TM1_{L53}TM1K2_{162}$ were prepared and purified as described in Ch. II. Iodide ion quenching was assessed using constant-ionic strength procedures and the averages from 2 independent experiments are shown. The membrane-bound integration intermediates were examined both before (▲) and after (⬟) the addition of MLT (5 μM final concentration). The data shown are the average of 2 independent experiments.

through the ribosomal tunnel, the lumenal end of the pore closed and the cytosolic end opened (Liao et al., 1997). Translocon gating was reversed when the second TMS moved through the tunnel. The cytosolic end of the pore closed and lumenal end opened (Table 9). The results from these experiments are in agreement with those obtained during the study of $2TM_{L53}K2$ (Ch. III), when two unique TMSs were present in the protein. Therefore, the ribosome does appear to differentiate between two adjacent TMSs having the same sequence and elicits an appropriate response at the membrane to ensure that the permeability barrier remains intact.

After studying the effects of native orientation and of identical TMS sequences on the bilayer, several conclusions can be made. The ribosome recognizes a nonpolar stretch of amino acids (19-23 residues in this study) as a TMS and elicits an appropriate response based on the order that each TMS is synthesized and enters the ribosomal tunnel. A partial TMS containing only 10 nonpolar residues was not sufficient to initiate changes in pore opening and closing. Reversing the orientation and order of the TMSs used in this study did not appear to affect the translocon gating mechanism. The entry of a TMS into the ribosomal tunnel seems to be the critical factor in eliciting changes at the membrane.

CHAPTER VI

DISCUSSION AND SUMMARY

The purpose of a membrane is to form a barrier between two aqueous compartments. The endoplasmic reticulum (ER) membrane separates an interior compartment, the lumen, from the surrounding cytoplasm. Since the lumen serves as a site of calcium ion storage in the cell, it is essential that the permeability barrier of the ER membrane be maintained to prevent the unregulated release of calcium ions. Protein synthesis of multi-spanning membrane proteins (MSMP) begins on free ribosomes located in the cytoplasm. MSMPs have hydrophilic domains that are located on both sides of the membrane as well as hydrophobic domains that need to be integrated into the membrane. How, then, are these membrane proteins able to be cotranslationally integrated into the bilayer of the ER membrane without disrupting the permeability barrier and allowing unregulated release of ions?

The cotranslational integration of MSMPs into the ER membrane is a highly regulated process involving extensive communication between the ribosome synthesizing the protein and the translocon of the ER membrane. During the cotranslational integration process it is the ribosome, not the translocon, that first recognizes a transmembrane segment (TMS) and initiates a series of conformational changes that occur at the ER membrane (Haigh and

Johnson, 2002; Liao et al., 1997; Woolhead et al., 2004). The nascent polypeptide is threaded into the aqueous translocon pore where each successive TMS is moved laterally through the translocon into the nonpolar core of the bilayer. The hydrophilic polypeptide segments on each side of the TMS are directed, alternatively, into either the aqueous cytosol or the aqueous lumen.

Here fluorescence spectroscopy was used to examine the process in which the permeability barrier of the ER membrane is maintained during the synthesis and subsequent integration of sequential TMSs of a MSMP. We were able to directly detect the exposure of the nascent chain to the cytosol and the lumen by monitoring the fluorescence intensity of a probe incorporated into the nascent chain. By varying the lengths of nascent chain being studied, we were able to examine and draw conclusions about the different stages of the integration process.

It was found that the translocon pore alternately opens and closes as sequential TMSs are synthesized and move into the ribosomal tunnel. While the first TMS through the tunnel caused the ribosome-translocon junction to open (Haigh and Johnson, 2002; Liao et al., 1997), the second TMS elicited both the closure of this junction and the opening of the lumenal end of the pore. The collisional quenching data show that when TMS2 first entered the ribosomal tunnel, the ribosome did not immediately recognize the nascent polypeptide as a second TMS, and maximal quenching by cytosolic I^- was observed ($2TM_{L12}K2_{122}$). However, after the C-terminal end of TMS2 had moved 7

residues from the PTC, changes at the membrane had occurred. The ribosome-translocon junction was reformed and the lumenal end of the translocon pore was opened, as shown by the maximal quenching of lumenal I^- ($2TM_{L12}K2_{126}$). Thus, the ribosome recognizes a newly synthesized TMS and effects changes at the membrane early on during translation, when the TMS is located just 4-7 residues from the PTC.

The synthesis and entry of a third TMS into the ribosomal tunnel reversed the changes that had occurred at the membrane during the synthesis of TMS2. The nascent chain remained protected from the cytosol after TMS3 had entered the tunnel and was located 3 residues from the PTC ($3TM_{L12,17}K3_{159}$). After TMS3 moved an additional 3 residues from the PTC, the nascent chain was no longer protected from the cytosol because maximal quenching by cytosolic I^- was observed ($3TM_{L12,17}K3_{162}$).

The presence of a TMS appears to be the critical factor in effecting pore opening/closing. When only one half of a TMS was present ($2TM_{L53}K1.5$), the ribosome did not recognize the 10 residue hydrophobic stretch as a TMS and did not initiate the integration progress. The ribosome also did not distinguish between TMSs based on their orientation in the bilayer ($TM2_{L53}TM1$). When two identical TMSs were synthesized in series ($TM1_{L53}TM1$), the ribosome identified each stretch of hydrophobic amino acids as a TMS and elicited a different response based on their order of entry into the tunnel. Therefore, the ribosome seems to effect alternating pore closure when a sufficiently-long stretch of

hydrophobic amino acids, recognized as a TMS, is synthesized and moves down the ribosomal tunnel.

The changes effected at the translocon by the synthesis of multiple TMSs do not correlate with nascent chain length. Increasing the length of the nascent chain loop between adjacent TMSs ($2TM_{L53}K2$ and $3TM_{L12,67}K3$) did not alter the pattern observed. When each newly synthesized TMS had entered the tunnel and was located 4-7 residues from the PTC, changes in translocon gating occurred. Therefore, it is most likely the position of the TMS inside the ribosome, not the length of nascent chain, that elicits pore opening/closing.

Liao et al. (Liao et al., 1997) hypothesized that the ribosome may recognize a TMS when a weakly nonpolar patch in the ribosomal tunnel nucleates the folding of a hydrophobic TMS into an α-helix. To address this hypothesis, FRET experiments were performed using a protein containing a single TMS. The results showed that the TMS does fold into an α-helix, or nearly so, while far inside the ribosomal tunnel (Woolhead et al., 2004). No folding was observed when the nascent chain lacked a TMS, or when, in the absence of microsomes, the TMS was located outside of the ribosome (Lin, unpublished data; Woolhead et al., 2004). FRET experiments have since been performed with the MSMPs used in the collisional quenching studies described in this dissertation (Lin, unpublished data), and it was found that the changes observed in translocon gating exactly coincided with ribosome-induced TMS

folding. Thus, nascent chain folding and binding far inside the tunnel control ribosome-translocon interactions at the ER membrane.

The data obtained studying MSMPs containing 2 and 3 TMSs reveal that the synthesis and movement of sequential TMSs into the ribosomal tunnel elicit changes at the membrane that cause the translocon pore to alternately open and close. These observations seem reasonable because the MSMPs contain alternating aqueous lumenal and cytoplasmic domains that need to be directed into the lumen and cytoplasm respectively. The integrity of the ER membrane is maintained during the cotranslational integration of MSMPs by ensuring that one end of the translocon pore remains sealed at any given time. The data reveal that cotranslational integration of a MSMP is a well choreographed and precisely timed event necessary to maintain the integrity of the ER membrane.

REFERENCES

Alder, N. N., and Johnson, A. E. (2004). Cotranslational membrane protein biogenesis at the endoplasmic reticulum. J Biol Chem *279*, 22787-22790.

Alder, N. N., and Johnson, A. E. (2008). Fluorescence Mapping of Mitochondrial TIM23 Complex Reveals a Water-Facing, Substrate-Interacting Helix Surface. Cell *134*, 439-450.

Alder, N. N., Shen, Y., Brodsky, J. L., Hendershot, L. M., and Johnson, A. E. (2005). The molecular mechanisms underlying BiP-mediated gating of the Sec61 translocon of the endoplasmic reticulum. J Cell Biol *168*, 389 - 399.

Ban, N., Nissen, P., Hansen, J., Moore, P. B., and Steitz, T. A. (2000). The complete atomic structure of the large ribosomal subunit at 2.4 A resolution. Science *289*, 905-920.

Beckman, R., Bubeck, D., Grassucci, R., Penczek, P. A., and Verschoor, A. (1997). Alignment of conduits for the nascent polypeptide chanin in the ribosome-Sec61 complex. Science *278*, 2123-2126.

Beckman, R., Spahn, C. M. T., Penczek, P. A., Sali, A., Frank, J., and Blobel, G. (2001). Architecture of the protein-conducting channel associated with the translating 80S ribosome. Cell *107*, 361-372.

Berridge, M. J. (2002). The endoplasmic reticulum: a multifunctional signaling organelle. Cell Calcium *32*, 235-249.

Blobel, G., and Dobberstein, B. (1975). Transfer of proteins across membranes. I. Presence of proteolytically processed and unprocessed nascent

immunoglobulin light chains on membrane-bound ribosomes of murine myeloma. J Cell Biol *67*, 835-851.

Blobel, G., (1999) http://nobelprize.org/nobel_prizes/medicine/laureates/1999/illpres/protein.html

Blobel, G., and Sabatini, D. D. (1970). Controlled proteolysis of nascent polypeptides in rat liver cell fractions. I. Location of the polypeptides within ribosomes. J Cell Biol *45*, 130-145.

Breyton, C., Haase, W., Rapoport, T. A., Kuhlbrandt, W., and Collinson, I. (2002). Three-dimensional structure of the bacterial protein-translocation complex SecYEG. Nature *418*, 662-665.

Brogden, K. A. (2005). Antimicrobial peptides: pore formers or metabolic inhibitors in bacteria? Nature Reviews Microbiology *3*, 235-250.

Cranney, M., Cundall, R. B., Jones, G. R., Richards, J. T., and Thomas, E. W. (1983). Fluorescence lifetime and quenching studies on some interesting diphenylhexatriene membrane probes. Biochim Biophys Acta *735*, 418-425.

Crick, F. (1970). Central dogma of molecular biology. Nature *227*, 561-563.

Crowley, K. S., Liao, S., Worrell, V. E., Reinhart, G. D., and Johnson, A. E. (1994). Secretory proteins move through the endoplasmic reticulum membrane via an aqueous, gated pore. Cell *78*, 461-471.

Crowley, K. S., Reinhart, G. D., and Johnson, A. E. (1993). The signal sequence moves through a ribosomal tunnel into a noncytoplasmic aqueous environment at the ER membrane early in translocation. Cell *73*, 1101 - 1115.

Demaurex, N., and Frieden, M. (2003). Measurements of the free lumenal ER Ca^{+2} concentration with targeted "chameleon" fluorescent proteins. Cell Calcium *34*, 109-119.

Denning, K., (2006) http://www.yorku.ca/kdenning/++2140%202006-7/2140-17oct2006.htm

Do, H., Falcone, D., Lin, J., Andrews, D. W., and Johnson, A. E. (1996). The cotranslational integration of membrane proteins into the phospholipid bilayer is a multistep process. Cell *85*, 369-378.

Engelman, D. M., and Steitz, T. A. (1981). The spontaneous insertion of proteins into and across membranes: the helical hairpin hypothesis. Cell *23*, 411-422.

Erickson, A. H., and Blobel, G. (1983). Cell-free translation of messenger RNA in a wheat germ system. Methods Enzymol *96*, 38-50.

Fujiki, Y., Hubbard, A. L., Fowler, S., and Lazarow, P. B. (1982). Isolation of intracellular membranes by means of sodium carbonate treatment: application to endplasmic reticulum. J Cell Biol *93*, 97-102.

Gilmore, R., Blobel, G., and Walter, P. (1982a). Protein translocation across the endplasmic reticulum. I. Detection in the microsomal membrane of a receptor for the signal recognition particle. J Cell Biol *95*, 463-469.

Gilmore, R., Walter, P., and Blobel, G. (1982b). Protein translocation across the endoplasmic reticulum. II. Isolation and characterization of the signal recognition particle receptor. J Cell Biol *95*, 470-477.

Grimes, W. and Lapointe, M. (2002) http://www.biology.arizona.edu/cell_bio/

problem_sets/membranes/graphics/proteins.jpg

Gumbart, J., and Schulten, K. (2006). Molecular dynamics studies of the archaeal translocon. Biophys J *90*, 2356-2367.

Haider, S., Hall, B. A., and Sansom, M. S. (2006). Simulations of a protein translocation pore: SecY. Biochemistry *45*, 13018-13024.

Haigh, N. G., and Johnson, A. E. (2002). A new role for BiP: closing the aqueous translocon pore during protein integration into the ER membrane. J Cell Biol *156*, 261 - 270.

Hamman, B. D., Chen, J. C., Johnson, E. E., and Johnson , A. E. (1997). The aqueous pore through the translocon has a diameter of 40-60 angstroms during cotranslational translocation at the ER membrane. Cell *89*, 535-544.

Hamman, B. D., Hendershot, L. M., and Johnson , A. E. (1998). BiP maintains the permeability barrier of the ER membrane by sealing the lumenal end of the translocon pore before and early in translocation. Cell *92*, 747-758.

Holmes, S. (2007) http://www-stat.stanford.edu/~susan/courses/s166/central.gif

Johnson, A. E., and van Waes, M. A. (1999). The translocon: a dynamic gateway at the ER membrane. Annu Rev Cell Dev Biol *15*, 799-842.

Katsu, T., Ninomiya, C., Kuroko, M., Kobayashi, H., Hirota, T., and Fujita, Y. (1988). Action Mechanism of amphipathic peptides gramicidin S and melittin on erythrocyte membrane. Biochim Biophys Acta *939*, 57-63.

Knoll, A. H. (1992). The early evolution of eukaryotes: a geological perspective. Science *256*, 622-627.

Koch, G. L. (1990). The endoplasmic reticulum and calcium storage. Bioessays *12*, 527-531.

Krieg, U. C., Johnson, W. E., and Walter, P. (1989). Protein translocation across the endoplasmic reticulum membrane: identification by photocross-linking of a 39 kD integral membrane glycoproteins as part of a putative translocation tunnel. J Cell Biol *109*, 2033-2043.

Ladokhin, A. S., Selsted, M. E., and White, S. H. (1997). Sizing membrane pores in lipid vesicles by leakage of co-encapsulated markers: pore formation by melittin. Biophys J *72*, 1762-1766.

Liao, S. (1997). unpublished data. Texas A&M University, c/o Art Johnson (ajohnson@medicine.tamhsc.edu).

Liao, S. L., Lin, J., Do, H., and Johnson, A. E. (1997). Both lumenal and cytosolic gating of the aqueous ER translocon pore are regulated from inside the ribosome during membrane protein integration. Cell *90*, 31 - 41.

Lin, P. J. (2008). unpublished data. Texas A&M University, c/o Art Johnson (ajohnson@medicine.tamhsc.edu).

Manting, E. H., van Der Does, C., Remigy, H., Engel, A., and Driessen, A. J. (2000). SecYEG assembles into a tetramer to form the active protein translocation channel. EMBO J *19*, 852-861.

Matsuzaki, K., Yoneyama, S., and Miyajima, K. (1997). Pore formation and translocation of melittin. Biophys J *73*, 831-838.

McCormick, P. J., Miao, Y., Shao, Y., Lin, J., and Johnson, A. E. (2003). Cotranslational protein integration into the ER membrane is mediated by the binding of nascent chains to translocon proteins. Molecular Cell *12*, 329-341.

Menetret, J.-F., Hegde, R. S., Heinrich, S. U., Chandramouli, P., Ludtke, S. J., Rapoport, T. A., and Akey, C. W. (2005). Architecture of the ribosome-channel complex derived from native membranes. J Mol Biol *348*, 445-457.

Menetret, J.-F., Neuhof, A., Morgan, D. G., Plath, K., Radermacher, M., Rapoport, T. A., and Akey, C. W. (2000). The structure of ribosome-channel complexes engaged in protein translocation. Mol Cell *6*, 1219-1232.

Meyer, D. I., Krause, E., and Dobberstein, B. (1982). Secretory protein translocation across membranes - the role of the 'docking protein'. Nature *297*, 647-650.

Morgan, D. G., Menetret, J.-F., Neuhof, A., Rapoport, T. A., and Akey, C. W. (2002). Structure of the mammalian ribosome-channel complex at 17A resolution. J Mol Biol *324*, 871-886.

Naito, A., Nagao, T., Norisada, K., Mizuno, T., Tuzi, S., and Saito, H. (2000). Confirmation and dynamics of melittin bound to magnetically oriented lipid bilayers by solid state 31P and 13C NMR spectroscopy. Biophys J *78*, 2405-2417.

Nichitta, C. V., and Blobel, G. (1990). Assembly of translocation-competent proteoliposomes from detergent-solubilized rough microsomes. Cell *60*, 259-269.

Osborne, A. R., Rapoport, T. A., and van den Berg, B. (2005). Protein translocation by the Sec61/SecY channel. Annu Rev Cell Dev Biol *21*, 529-550.

Ramachandran, R., Tweten, R. K., and Johnson, A. E. (2004). Membrane-dependent conformational changes initiate cholesterol-dependent cytolysin oligomerization and intersubunit B-strand alignment. Nat Struct Mol Biol *11*, 697-705.

Rapiiejko, P. J., and Gilmore, R. (1997). Empty site forms of the SRP54 and SRa GTPases mediate targeting of ribosome-nascent chain complexes to the endoplasmic reticulum. Cell *89*, 703-713.

Rapoport, T. A. (2007). Protein translocation across the eukaryotic endoplasmic reticulum and bacterial plasma membranes. Nature Reviews *450*, 663-669.

Rapoport, T. A., Goder, V., Heinrich, S. U., and Matlack, K. E. S. (2004). Membrane-protein integration and the role of the translocation channel. Trends in Cell Biology *14*, 568-575.

Rapoport, T. A., Jungnickel, B., and Kutay, U. (1996). Protein transport across the eukaryotic endoplasmic reticulum and bacterial inner membranes. Annu Rev Biochem *65*, 271-303.

Sansom, M. P. (1991). The biophysics of peptide models of ion channels. Prog Biophys Mol Biol *55*, 139-215.

Saparov, S. M., and al., e. (2007). Determining the conductance of the SecY protein translocation channel for small molecules. Mol Cell *26*, 501-509.

Tian, P., and Andricioaei, I. (2006). Size, motion, and function of the SecY translocon revealed by molecular dynamics simulations with virtual probes. Biophys J *90*, 2718-2730.

van den Berg, B., Clemons, W. M., Collinson, I., Modis, Y., Hartmann, E., Harrison, S. C., and Rapoport, T. A. (2004). X-ray structure of a protein-conducting channel. Nature *427*, 662-664.

van den Ent, F., and Lowe, J. (2006). RF cloning: A restriction-free method for inserting target genes into plasmids. Journal of Biochemical and Biophysical Methods *67*, 67 - 74.

Vogel, H., and Jahnig, F. (1986). The structure of melittin in membranes. Biophys J *50*, 573-582.

von Heijne, G. (1985). Signal sequences: the limits of variation. J Mol Biol *184*, 99-105.

Walter, P., and Blobel, G. (1983). Preparation of microsomal membranes for cotranslational protein translocation. Methods Enzymol *96*, 84-93.

Walter, P., and Johnson, A. E. (1994). Signal sequence recognition and protein targeting to the endoplasmic reticulum membrane. Annu Rev Cell Dev Biol *10*, 87-119.

Walter, P., and Lingappa, V. R. (1986). Mechanism of protein translocation across the endoplasmic reticulum membrane. Annu Rev Cell Dev Biol *2*, 499-516.

Wolin, S. L., and Walter, P. (1988). Ribosome pausing and stacking during translation of a eukaryotic mRNA. EMBO J *7*, 3559-3569.

Woolhead, C. A., McCormick, P. J., and Johnson, A. E. (2004). Nascent membrane and secretory proteins differ in FRET-detected folding far inside the ribosome and in their exposure to ribosomal proteins. Cell *116*, 725 - 736.

VITA

NAME:	Candice Gene Jongsma
EDUCATION:	B.S., Chemistry April, 2002 Grand Valley State University
	B. S., Biology April, 2002 Grand Valley State University
	Ph. D., Chemistry Texas A&M University December, 2008
PERMANENT ADDRESS:	Dept. of Chemistry c/o Dr. Art Johnson Texas A&M University College Station, TX 77843-3255
EMAIL ADDRESS:	cjongsma@mail.chem.tamu.edu